Depositional evolution of La Parra kasrtic lake (Iberian Chain, Spain) during the last 1,600 years: Climate and human impact implications

Fernando Barreiro-Lostres

Trabajo Fin de Máster

Máster de Iniciación a la Investigación en Geología

Curso 2011-2012

“Lakes are dynamic response systems collecting complex signatures of the landscape (vegetation, carbon, pollen, dust, ash, soil erosion, floods, seasons) and aquatic systems (water source, composition, balance, temperature, chemistry, isotopes, carbon, precipitates, biotic and abiotic processes). These signatures integrate climate parameters of temperature, precipitation, wind, seasonality, climate extremes, and variability”

(Kerry Kelts)

Index

ABSTRACT

Lake La Parra (39º 50.948', 1º 52', 1014 m) is a small, relatively deep (Zmax = 17.5 m), freshwater monomictic lake with a circular morphology and a diameter of 116 m It is part of a karstic lake complex of seven lakes located in the Iberian Range (Cuenca, East of Spain), and it has been developed in a sinkhole that intercepted the main regional aquifer.

The sedimentary record of the deepest part of the lake, analysed using sedimentological, microscopic, geochemical and physical techniques is mainly constituted by clastic carbonated sediments, characterized by a high variability of sedimentary facies, which is controlled mainly by changes in the detritic input. At same time, these fluctuations reflect a wide hydrological variability along the last 1600 years. The chronological model for the sediment sequence is based on 7 AMS ^{14}C dates.

The depositional history of Lake La Parra comprises five stages: (i) The onset of lacustrine sedimentation around 300 cal. yr AD; (ii) a shallow to deep lake during the Dark Ages (500 - 900 cal. yr AD); (iii) lower lake levels with increase in detritic input, coincident with the Medieval Climate Anomaly; (iv) a period of generally higher lake levels with development of frequent meromixis but with some low lake level phases during the Little Ice Age (1400 - 1850 cal. yr. AD); and (v) a slight increase of lake levels on recent times (1900-nowadays), preceded by an initial period of lower levels during the late 19th century.

The main human impact in the lake and the watershed environment is related to changes in the land uses during the Middle Ages due to agriculture and transhumation that increased sediment delivery to the lake, and more recently the use of groundwater from regional aquifer for agricultural purposes.

The paleohydrological-paleoclimate reconstructions of Lake La Parra are coherent with other paleoclimate archives of the Iberian Peninsula showing a more arid MCA and more humid LIA in the western Mediterranean. These new finding also support the hypothesis of an east-west climate see-saw in the Mediterranean region since 900 AD.

Key-words: Late Holocene, sedimentary facies, geochemistry, Iberian Peninsula, karstic lake, lacustrine depositional environments, palaeohydrology, sedimentary facies, X-Ray Fluorescence.

RESUMEN

La laguna de La Parra (39º 50.948', 1º 52', 1014 m) es un lago pequeño relativamente profundo (Zmax = 17.5 m) de agua dulce, monomíctico y con morfología circular (116 m diámetro). Forma parte de un complejo kárstico constituido por siete lagos situado en la Cordillera Ibérica (Cuenca, este de España), originado en una dolina que interceptó el acuífero regional.

El registro sedimentario de la zona más profunda del lago se ha estudiado mediante técnicas sedimentológicas, microscópicas, geoquímicas y físicas. Está constituido principalmente por sedimentos clásticos carbonatados, caracterizados por una gran variabilidad de facies sedimentarias que están controladas por cambios en la entrada de detríticos al sistema. Al mismo tiempo, estas fluctuaciones reflejan una amplia variabilidad hidrológica durante los últimos 1600 años. El modelo cronológico de la secuencia sedimentaria se basa en 7 dataciones de 14C AMS.

La historia sedimentaria de la laguna de La Parra comprende 5 etapas: (i) el comienzo de la sedimentación lacustre hacia el año 300 DC; (ii) un lago somero que aumenta progresivamente su nivel durante la Baja Edad Media (500 – 900 DC); (iii) niveles del lago bajos, con aumento en los aportes detríticos coincidiendo con la Anomalía Climática Medieval (ACM); (iv) un periodo con predominio de niveles altos del lago, pero algún episodo de niveles bajos, con desarrollo de meromixis frecuente durante la Pequeña Edad del Hielo (PEH, 1400 . 1850 DC) y (v) un ligero aumento de los niveles del lago en

tiempos recientes (1900 - actualidad), precedido por un periodo inicial de bajo nivel de agua a finales del siglo XIX.

La principal afección antrópica en el lago y su entorno está relacionada con cambios en el uso de la tierra durante la Edad Media debido a la agricultura y la transhumancia, lo que implicó un aumento en los aportes detríticos al lago; y más recientemente, con la extracción de aguas subterráneas del acuífero regional mediante pozos agrícolas.

Las fluctuaciones paleohidrológicas y paleoambientales de la laguna de La Parra son coherentes con otros registros paleoclimáticos de la Península Ibérica, mostrando una fase más árida durante la ACM y más húmeda durante la PEH en el Mediterráneo occidental. Este nuevo aporte refuerza la hipótesis de un comportamiento antitético este-oeste del clima en la region mediterránea desde el 900 DC.

Palabras clave: Holoceno tardío, facies sedimentarias, geoquímica, Península Ibérica, lago kárstico, ambientes de sedimentación lacustre, paleohidrología, facies sedimentarias, Fluorescencia de Rayos X.

Introduction

The discovery during the last decades of periods of past rapid changes within the climate system (Mann, 2007) has demonstrated the high frequency variability of Earth's climate and the occurrence of variations from annual to millennial timescales. This variability is known to result from both internal and external factors, the latter associated with both natural and anthropogenic influences (Mann, 2007; Hegerl et al., 2011, Crowley, 2000). A number of natural processes besides the Earth-orbital changes as oscillations of the coupled atmosphere-ocean-ice sheet system, solar activity changes, volcanic greenhouse-gases emission, tectonics and relative location of continents and even meteoritic impacts control the climate system (Alley et al., 1997; Mann, 2007).

Over past two millennia, the main boundary conditions of the climate system (orography, orbital parameters and the spatial extent of continental ice sheets) have not changed significantly, so this time interval provides an appropriate context for estimating the envelope of natural climate variability. Although these variations have been smaller than those from past glacial - interglacial periods, they have deeply affected human societies, forcing people to develop subsistence strategies to overcome changing conditions. Since Neolithic times, environmental change has been a determinant factor in civilizations' fate and even in historical times, climate has greatly affected humankind (Turney et al., 2006). On the other hand, changes in human activities affect back climate's evolution at hemispheric scales, particularly since the industrial revolution (Houghton, 2001; Mann, 2007).

Instrumental records are too short to fully record the variability of the climate system. Quaternary palaeoclimatic archives often record more variability than typically observed instrumentally during this century, providing estimates of the past atmospheric composition, temperature, precipitation, vegetation, extension of glaciers, and past ocean circulation (Duplessy, 2005). Lacustrine records are an excellent high-resolution sedimentary archive of regional abrupt changes in climate (Batist and Chapron, 2008), including regional variations in hydrology (precipitation/evaporation ratios, flood events, changes in river input), climate-controlled weathering and sediment transport processes, human impact and even seismic activity on the lake catchment.

A number of Holocene climatic reconstructions in the Mediterranean have been performed using lacustrine multiproxies (isotopes, pollen, geochemistry, sedimentology) (e.g. Roberts et al., 2011). In the Iberian Peninsula, lakes occur in a large variety of geographic, climatic and ecologic settings. There are lakes in mountains originated by glacial activity (Enol, Sanabria); karstic lakes that owe their origin to exokarstic activity (Taravilla, Somolinos) or to dissolution of evaporites or carbonates: (Banyoles, Moncortes, Zoñar, Estanya); and ephemeral saline lakes in the Ebro, Duero and Tajo River Basin originated by combination of erosion and karstic processes (Bujaraloz salt lakes) (González-Sampériz et al., 2008). The most significant Late Holocene climatic abrupt changes described in these sequences are the Ibero-Roman Humid Period, the Medieval Climate Anomaly and the Little Ice Age ((Moreno et al. 2009);(Morellón et al. 2009); (Martín-Puertas et al. 2009); (Corella et al. 2010); (Valero-Garcés and Moreno 2011); (Currás et al. 2012)).

In this work, high-resolution sedimentological, mineralogical and geochemical studies carried out on short gravity cores and long piston cores from La Parra Lake, a small karstic lake in the Iberian Range (central Spain) provide a detailed record of main depositional and hydrological changes during the last 1.600 cal. years in this region of the Iberian Range. The relatively high area/depth ratio of the lake basin amplifies the record of the local hydroclimatic variability, which is expected to be affected by climate and the well-known human impact in the area (grazing, crops, and fires) since Medieval times. The sedimentary facies and geochemical data together with a robust chronological model, provided by AMS radiocarbon dating techniques, have allowed disentangling the changing environmental conditions surrounding the lake and its watershed and the complex interplay between climate and human activities since the end of the Roman Period.

Regional setting

Study site

In the Iberian Peninsula there are large carbonate-dominated regions where endo and exo-karstic processes have been very active during the Quaternary. As a consequence, a number of lake basins have developed, mainly in tufa-dammed valleys and dolines. Particularly, in the Iberian Range, thick dolomitic Jurassic and Middle and Upper Cretaceous dolomitic formations have been affected by intense karstic processes (Alonso, 1986; Gutiérrez and Valverde, 1994; Carmona and Bitzer, 2001; Peña and Lozano, 2004) originating small funnel-shaped depressions, relatively deep that sometimes intercept the surrounding aquifers, developing karstic lakes (Valero-Garcés and Moreno 2011).

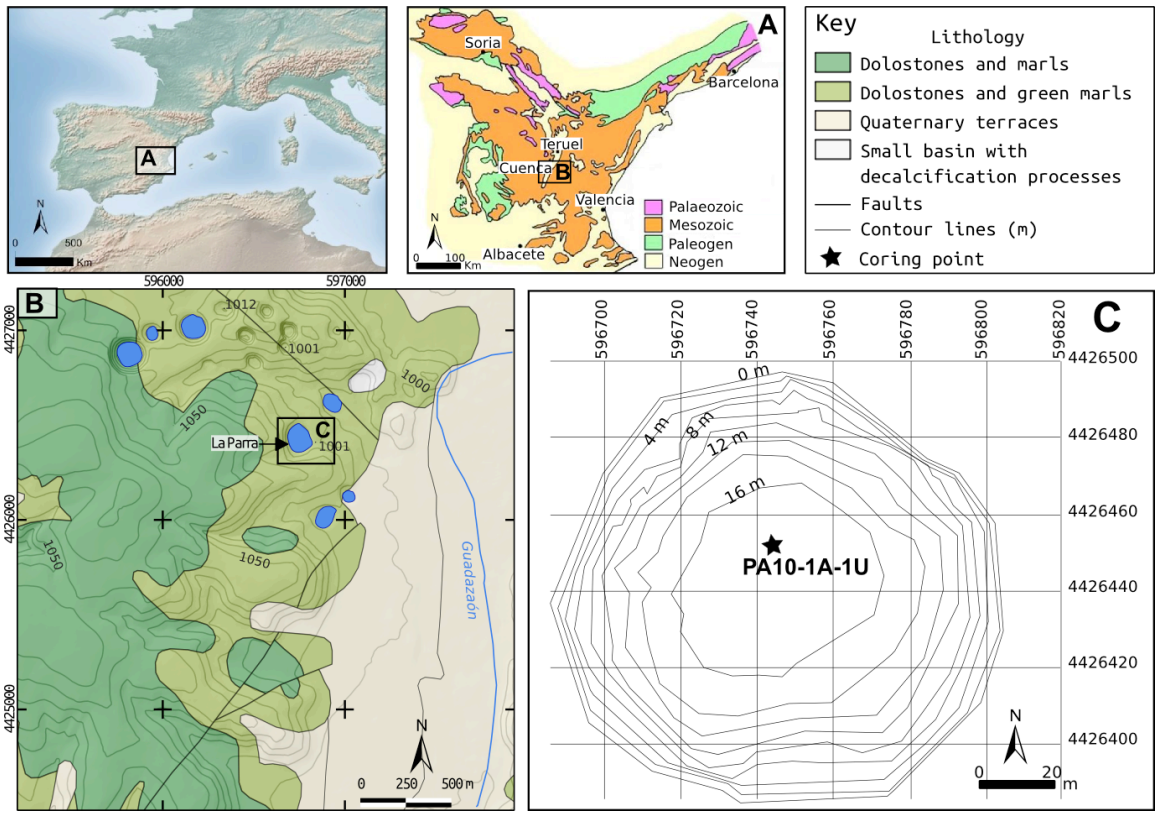

Fig. 1: *A - Location of the study area and geological scheme of the Iberian Range. B - Detailed geological map of the surroundings of La Parra lake (see legend at the right-top side (based on Ramírez del Pozo et al., 1973) and national topographical map (IGN, 2002). C - La Parra lake's bathymetry and location of studied core.*

La Parra lake is located on the western branch of the Iberian Range (Central - Eastern Spain). It belongs to the karstic lake complex of Cañada del Hoyo (Fig. 1), formed on Upper Cretaceous limestones and dolostones (Cenomanian-Turonian) but affecting as well Late Jurassic materials as Weald and Utrillas facies, composed of massive beds up to 2 m thick, lying sub-horizontally above Middle/Upper-Cenomanian green marls (correlated with Margas de Chera Formation, Segura et al., 1988). The origin of this complex is probably structural, following the NE-SW trace of the known Guadazaón polje, which follows the orientation of the Valdemoro fault (Eraso et al. 1979).

Geomorphology

The Guadazaón polje is one of the main morphological features on the study area, characterized as an open, elongated NE-SW trending depression (Fig. 2). The polje is developed on a slightly deformed surface that corresponds to the Pliocene Main Erosion

Surface of the Iberian Chain (which presents a faint inclination towards the SE of 1%), affecting carbonatic Cenomanian-Turonian formations and more clastic (Weald and Utrillas) Cretaceous formations (Gutiérrez and Valverde, 1994). The Utrillas Formation constitutes the base level of the polje. From a climatic point of view, this polje can be classified as a *Mediterranean-type*, but considering its evolution and morphology (progressive trend to subdivision), Peña et al. (1989) define it as an *Iberian-type* polje.

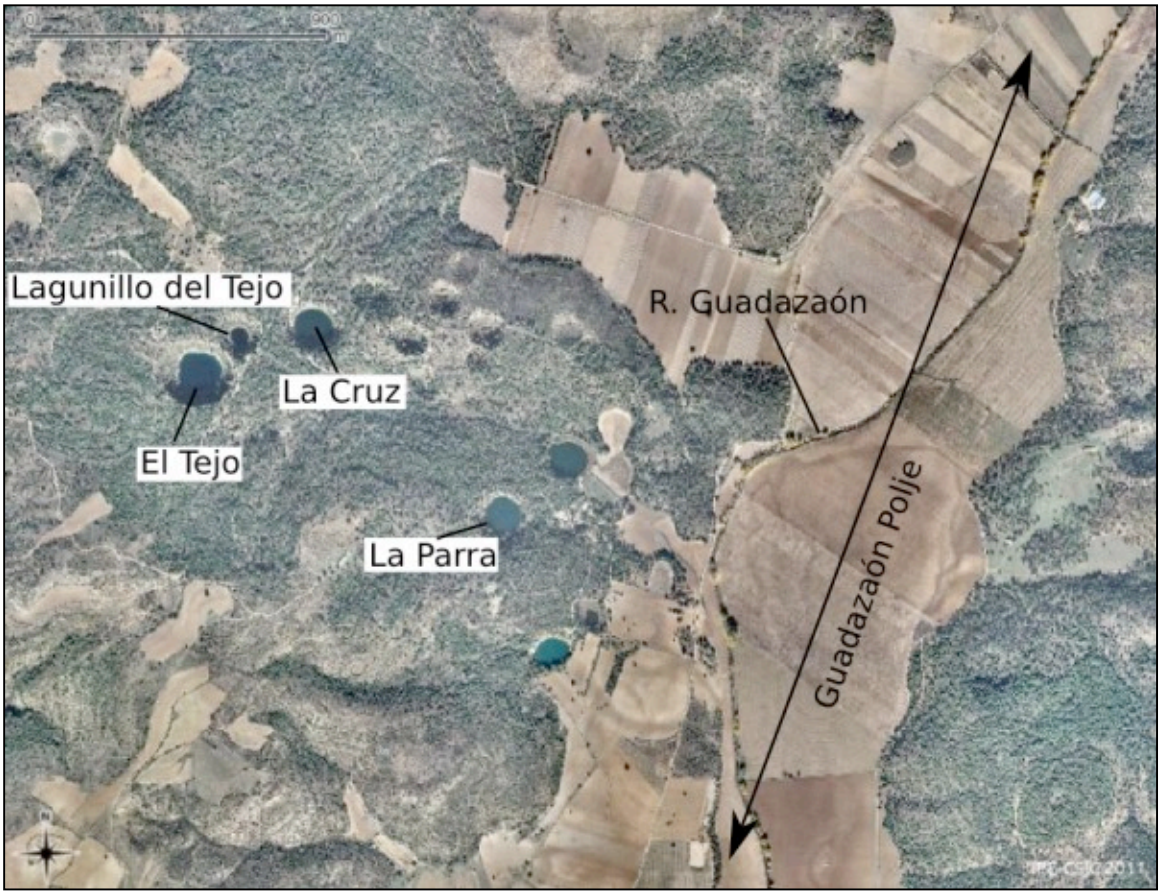

Fig. 2: Aerial orthophotograph of the study site showing the Guadazaón polje and the location of the karstic doline system in both margins. Only western margin present dolines with water.

In the Late Quaternary, the polje was captured by the actual fluvial system (Gutiérrez y Valverde, 1994). The Guadazaón River has deposited silts and red clays with angular cuarzitic and carbonatic pebbles on the bottom of the polje. Along the scarps, small alluvial fans occur, as well as tufa deposits associated to springs in the contact between Upper Cretaceous limestones-dolostones and the sandy Utrillas formation.

Near Cañada del Hoyo village and over the Main Erosion Surface a complex doline system developed. Although they are located on both margins of the Guadazaón polje, only some dolines situated on the right margin are flooded. One of these dolines is the lake La Parra. Related to their origin, some authors defend their genesis by dissolution processes facilitating by the diaclase net surrounding the dolines and their progressive widening (Alonso, 1986). Other authors as Eraso et al., 1979 explain their genesis by structural factors, particularly the occurrence of Jurassic and Cretaceous folds and fractures, responsible for the collapse of unkarstificable pre-Cenomanian materials (Utrillas and Weald facies) and dissolution of carbonatic deposits (Jurassic and Cenomanian limestones and dolostones) along preferential directions. More recently, Carmona and Bitzer (2001) argued that the regional NW-SE syncline affecting the Cretaceous has been a main factor in the development of these sinkholes by collapse as consequence of karstic dissolution.

Climate and vegetation

The Iberian Peninsula climate is influenced by both subtropical and the mid-latitude climatic dynamics. La Parra lake is located in a Mediterranean climatic context modulated by continental influences with sharp daily and seasonal temperature fluctuations. The mean annual precipitation in the study area is 542 mm, and the mean annual evapotranspiration has been estimated as 237 mm (Thornthwaite method; Custodio y Llamas, 1996; Escuder et al., 2009). The mean annual temperature is 14,6 ºC, ranging from 4 ºC (January) to 23 ºC (July) (Cuenca Meteorological Station, 12 Km NW of the lake). July is the driest month and October the wettest, with mean rainfall of 15,7 and 59,4 mm, respectively.

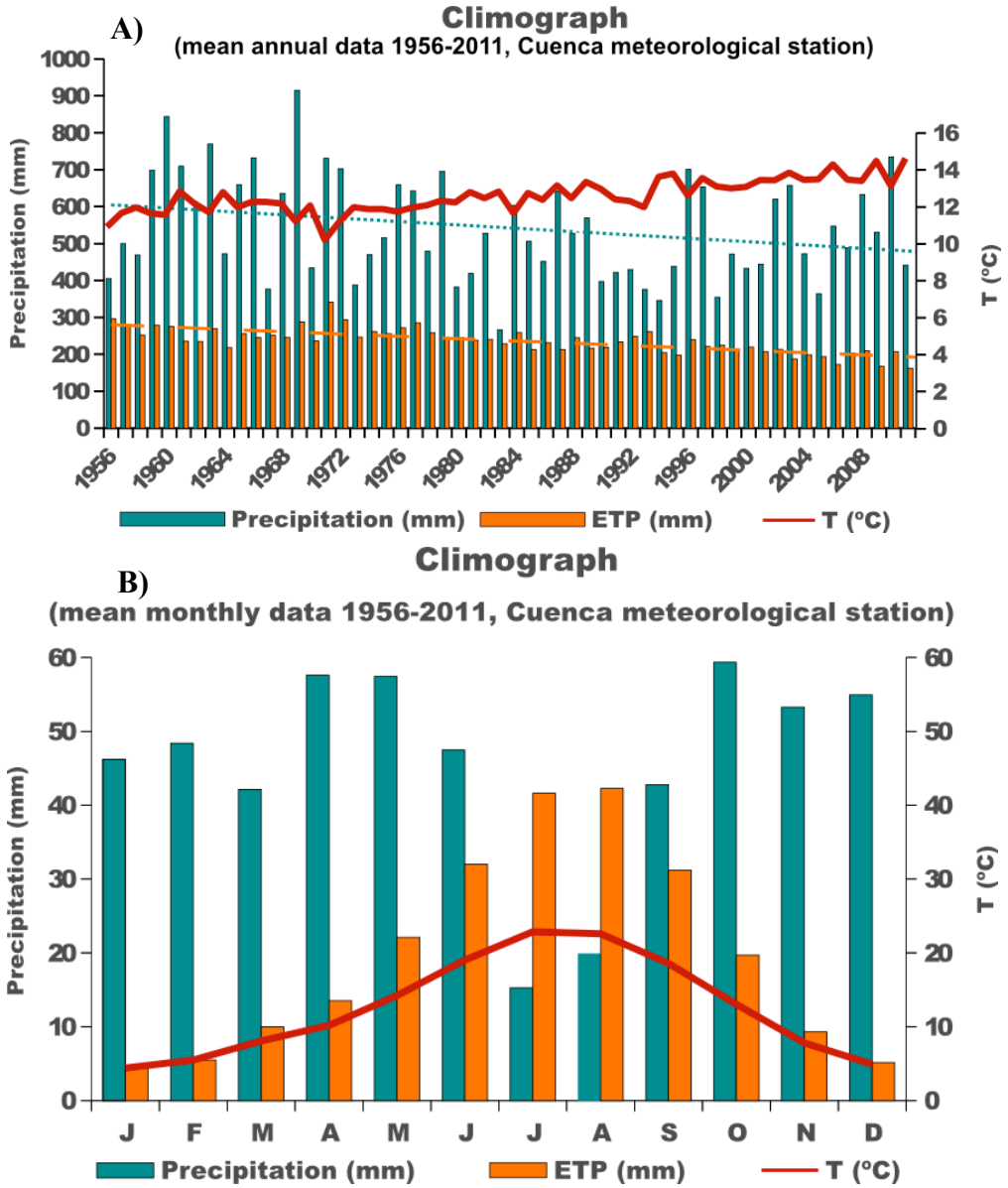

Fig. 3: A – Mean annual precipitation (mm), evapotranspiration (mm) and temperature (ºC) data of the study area. B - Mean monthly precipitation (mm), evapotranspiration (mm) and temperature (ºC) data. Data is derived from the Cuenca meteorological station, 12 Km NW of the lake, for the complete 1956-2011 period.

In figure 3A, a direct relation between precipitation and evapotranspiration is shown, with a lineal decrease from 1956 until 2011, ranging from 600 to 490 mm (P) and from 300 to 200 mm (ETP). This may be indicative of the synergetic response of the vegetation and the amount of rain. An increase of the mean annual temperature from about 11 ºC in 1956

to about 14ºC in 2011 is also clear, indicative of a warming of the region in 55 years of 3 ºC.

Figure 3B shows the distribution of precipitation through the year, with a maximum during autumn (more than 50 mm/month) and spring and with a minimum during summer, principally during July and August (less than 20 mm/month) when evapotranspiration may exceed rain inputs.

Bioclimatically, the area is located on the upper mesomediterranean horizon. The local vegetation is dominated by *Pinus nigra, Quercus faginea, Quercus ilex rotundifolia*, *Juniperus thurifera, Buxus sempervirens* and *Quercus coccifera* between others, showing the usual Mediterranean montane communities with some thermophytes (*Jasminum fruticans, Pistacia terebinthus*) and isolated mesophyllous taxa in humid locations (like *Corylus avellana* or *Tilia platyphyllo*s). Lower areas and flatlands are occupied by cereal crops. Due to human influence (recreational, introduction of exogenous species, ornamental pruning and grazing) a floral homogenization has occurred since 1990s (Escudero and Regato 1992). Currently the area is protected as a Natural Park.

Hydrology and limnology

In the area of Torcas de Cañada del Hoyo, seven lakes located on the right margin of Guadazaón polje – including La Parra Lake - contain water and are hydraulically connected with the groundwaters of the area. Hydrochemically, lakes waters present notorious differences with groundwaters, being bicarbonated-magnesian and high mineralized the formers and bicarbonated-calcic the latters. Isotopic studies (Carmona and Bitzer, 2001) have been demonstrated that these differences reflect the interactions between the strong effect of evaporation in the lakes and the continuous renovation of lakes waters by the input and output of groundwaters along fissures.

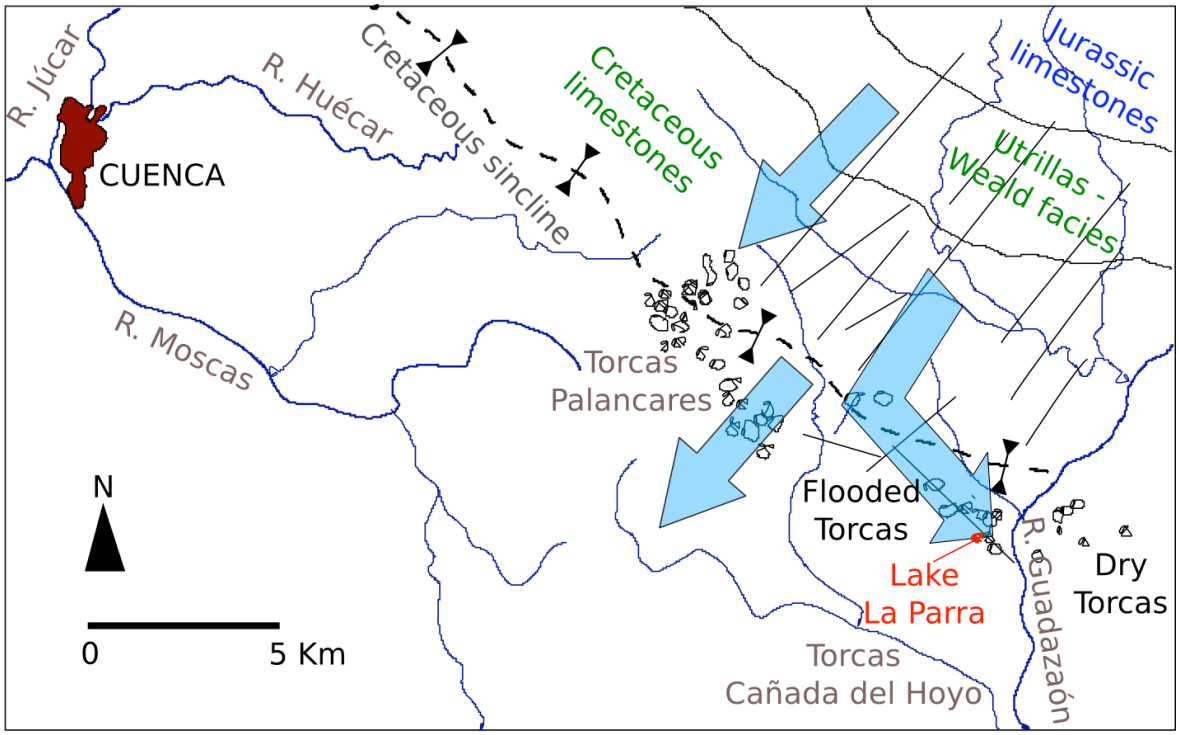

Fig. 4: Schematic map showing the occurrence of the sinkholes "Torcas" and their relation with the Cretaceous syncline, located on limestones and dolostones. Blue arrows indicate the flowing direction of regional groundwater, facilitated by NE-SW fractures (black lines). Modified from Carmona and Bitzer, 2001.

The recharge area for the aquifers feeding the lakes is located 15 Km N of the Cañada del Hoyo lakes, in an area of about 25 Km^2 composed of karstified Jurassic limestone

outcrops, called "*Tierra Muerta*", with an annual average precipitation of 650 mm. In these conditions, the effective recharge of the aquifer is estimated of 60 % of precipitation, generation a groundwater flux of about 300 L/s. Groundwaters flow towards the S reaching the lakes, and finally draining into the fluvial aquifer of Guadazaón river (Fig 4).

La Parra lake (39º5' N, 1º52' W, 1000 m a.s.l.) is one of these seven sinkholes, all with similar morphology and bedrock, but different hydrological and limnological behaviour, which leads to differences in the hydrochemistry. The lake is circular, with a diameter of 113 m and a total lake surface area of 10,012 m^2. The maximum depth is 17,5 m at the centre of the lake. There is not permanent inlet or surface outlet. The lake is mainly fed by groundwater from the surrounding local dolostone aquifer. A steep dolostone scarp encircles most of the lake, from the W to the SE.

The hydrology is controlled by: i) a relatively small catchment (~ 10 Ha); ii) a strong seasonality precipitation regime (Fig. 2); iii) a high evaporation rate and iv) recent water extraction wells for agricultural purposes in the main karstic regional aquifer, which has caused large variations on regional water-table levels affecting the underground inputs. The lake is holomictic. Water analyses performed in 2010 show that lake water chemistry is dominated by bicarbonate (4,78 meq/L) and magnesium (3,96 meq/L), with a conductivity ranging from 305 at the surface to 356 µS/cm at 16 m depth. Alkalinity values range from 5.9 to 6.2 meq/L, and pH is about 8.

Lake basin comprises mainly four modern depositional environments: a narrow littoral platform, a steep talus area, an offshore transitional area and a small offshore distal area. Current conditions show a low-energy environment with small lake level fluctuations (2–3 m) related to the water-levels of the main regional aquifer and the fluctuations of the Guadazaón River.

Material and methods

During the field campaign, coordinates and depth data were acquired to obtain the bathymetric map of La Parra lake, using a Sonar Mite ® echosounder. Later, a TIN interpolation model was calculated with the HYPACK ® software, providing the final bathymetric map (see Fig. 1).

Two long parallel cores (PA10-1A-U of 6,93 m and PA10-1B-U, of 5,24 m) were recovered on the deepest part of the lake (17,5 m) in May 2010 with the IPE-CSIC UWITEC ® floating platform and piston-corer (Fig. 5). Four short gravity cores were also taken with the water-sediment interface preserved. Then in a coring campain during summer of 2011, 21 short cores were obtained, distributed in a mesh covering the whole lake. The cores were split in two halves and sedimentary facies were defined by both, macroscopic-visual description including colour, grain-size, sedimentary structures, fossil content, and microscopic smear slides observations.

Fig. 5: IPE-CSIC UWITEC ® floating platform in la Parra lake used to obtain the PA10-1A-U and PA10-1B-U long cores, with 6,92 and 5,24 m respectively.

Microscopic inspection at 50-100x magnification of selected samples provided qualitative information about sediment components and texture of the sedimentary facies, following the methodology established by Schnurrenberger et al. (2003). Microscopic study was completed by Scanning Electron Microscopy (SEM) of selected samples using a JEOL JSM-6400 coupled with an energy dispersive X-ray (EDAX), INCA 300 X-Sight, for elemental identification. Samples were dried and then gold-coated to avoid peak overlapping. SEM observations were made in conventional high vacuum SEM.

The cores were photographed using the CCD camera attached to the AVAATECH X-Ray Fluorescence (XRF) core scanner located at the University of Barcelona. Core-scanning data are widely applied to paleoclimate reconstructions on timescales ranging from seasonal to millions of years (Tjallingii et al., 2011). The X-ray fluorescence core scanner is a computer-controlled core-scanning tool that analyzes the chemical composition of sediments directly at the surface of a split sediment core (Fig. 6 up), consequently, the measurements are non-destructive and require very limited sample

preparation. Owing to the nature of the surface of splited surfaces, particularly effects resulting from sample inhomogeneity and surface roughness, results are semiquantitative, yet provide reliable records of the *relative variability* in elemental composition downcore (Richter et al., 2006). As consequence, is very important to reduce at maximum the possible physical inhomogeneities in a split core by cleaning carefully its surface. Heterogeneity and surface roughness effects could become more pronounced for coarser-grained sample material (Tjallingii, 2006).

In XRF core scanners, the incoming X-rays penetrate the sediment surface (Fig. 6 down) and ionize the elements within the sediment those subsequently emit their characteristic emission line energies (Tjallingii, 2006), which is recovered with the detector and transformed to a digital signal. Consequently, this signal depends of the main atomic composition of the excited area, so values are semiquantitative.

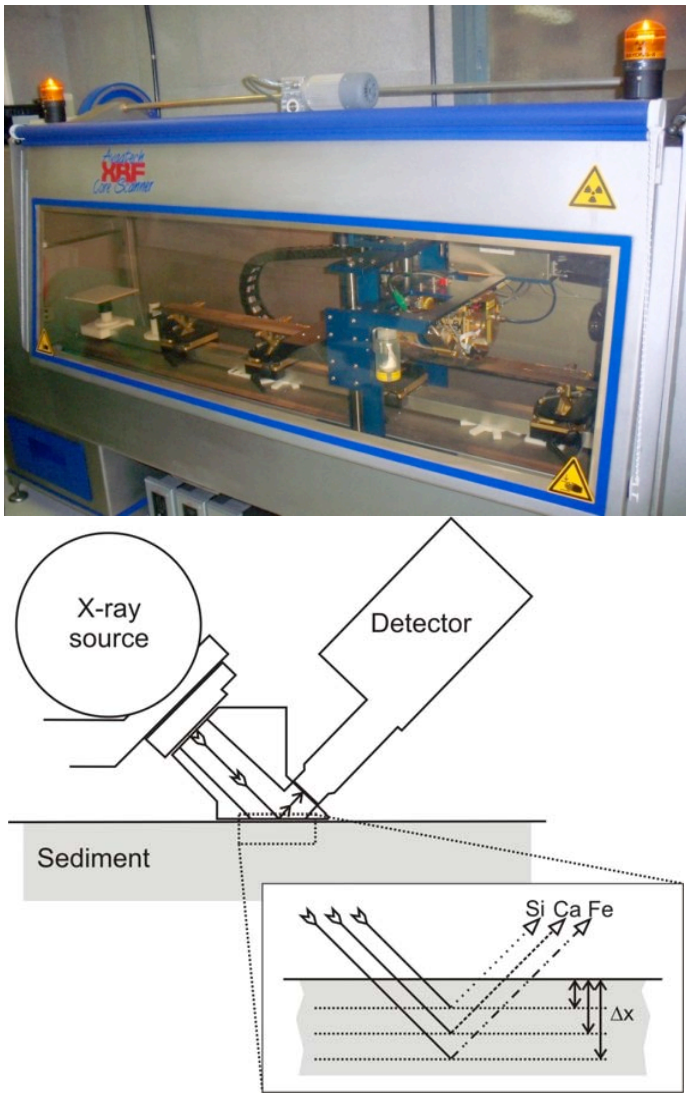

Fig. 6: Up) AVAATECH XRF scanner at the University of Barcelona. Down) Excitation geometry in XRF core scanner analysis (Tjallingii, 2006)

The longest core (PA10-1A-1U) was analysed using an X-ray current of 2000 μA, with two passes of 10 kV and 30 kV X-ray voltage at 15 s and 25 s count time respectively, and a spatial resolution of 5 mm. Following Richter et al. (2006) the data obtained by the XRF core scanner are expressed as element intensities (counts per second). Element concentrations are not directly available from the XRF measurements and the processing software, but the obtained values can be used as estimates of relative concentrations.

The same core was also sub-sampled every 2 cm (Fig. 7) for Total Organic Carbon (TOC), Total Inorganic Carbon (TIC) and Total Nitrogen (TN); every 10 cm for mineralogical analyses and for diatom study. TOC and TIC were measured in a LECO SC144 DR furnace while TN was measured using a VARIO MAX CN elemental analyser, both at the Instituto Pirenaico de Ecologia (IPE-CSIC) Laboratories.

Fig. 7: Sampling process of the different sedimentary proxies of the core PA10-1A-U.

The sediment mineralogy was characterized by X-ray diffraction with a Siemens D-500 diffractometer (Cu kα, 40 kV, 3 mA with a graphite monocromator) and relative mineral identification and abundance was determined using peak intensities following the standard procedures described by Chung (1974a, b).

The chronology for the lacustrine sequence is constrained by 9 Accelerator Mass Spectrometry (AMS) ^{14}C dates analysed at the Poznan Radiocarbon Laboratory (Poland). The dates are derived from terrestrial macro-remains. Radiocarbon dates were calibrated using CALIB REV 6.0.0 software (Stuiver and Reimer, 1993) and the INTCAL09 curve (Reimer et al., 2009) selecting the median of the 95.4% distribution (2σ probability interval).

Results

Modern Depositional Environments

Present-day sedimentary facies and depositional sub-environments in modern lake La Parra were described and interpreted based on 23 short-core sampling points (Fig. 9). The relatively small size of the lake, its topographically-closed watershed and its funnel-shaped morphology (Eraso et al, 1979) determine the present low-energy depositional environments and relatively small lake-level fluctuations (2 to 3 m). The modern lake could be described as a freshwater, relatively deep, carbonate-producing, monomictic lake.

According to sedimentological features, grain-size distribution and OM content, four main depositional sub-environments can be identified in the modern lake basin (Fig. 9): (i) the littoral platform; (ii) the talus area; (iii) the offshore, transitional area; and (iv) the offshore distal area.

(i) The 'littoral platform' constitutes a relatively flat, flooded area, partially colonized by vegetation that protects the littoral zones from waves, stabilizes the substrate, provides support for epiphytic fauna and contributes to the precipitation of carbonate particles around the plant stems. This sub-environment is better developed along the southern shores, which is characterized by gentle slopes, and it narrows until disappearing on the steeper scarps of the northern shore (Fig. 9), which is dominated by rock-fall processes.

(ii) The 'talus area' is a 2 to 10 m water depth zone, extending from the inner limit of the littoral vegetation belt to the offshore transitional area. It presents a steep scarp, which limits the presence of vegetation as a result of the lack of light and the occurrence of small mass movements as a result of talus destabilization. Sediment is composed mainly of brown dark matrix with white carbonatic pebbles (root casts, worm tracks and mixed sediment textures) fine (facies 2.1), medium (facies 2.2) and coarse (facies 2.3) sands with abundant plant remains. Coarser sands are associated with the input from an ephemeral creek located in the S part of the lake. Mass-wasting processes remobilize talus sediments and transport fine detrital material downslope to distal areas.

(iii) The 'offshore transitional area' (from 10 to 16 m water depth) is a wide area (> 80 m wide) characterized by a flat morphology. Sediments are light (facies 1.3A) and dark (facies 1.3B) grey coarse massive silts, with abundant small (< 4 mm) aquatic vegetal fragments and disperse white carbonatic pebbles (< 2 mm).

(iv) The 'offshore distal area' (from 16 to 17 m water depth) comprises a central, deepest, flat and narrow area (< 40 m

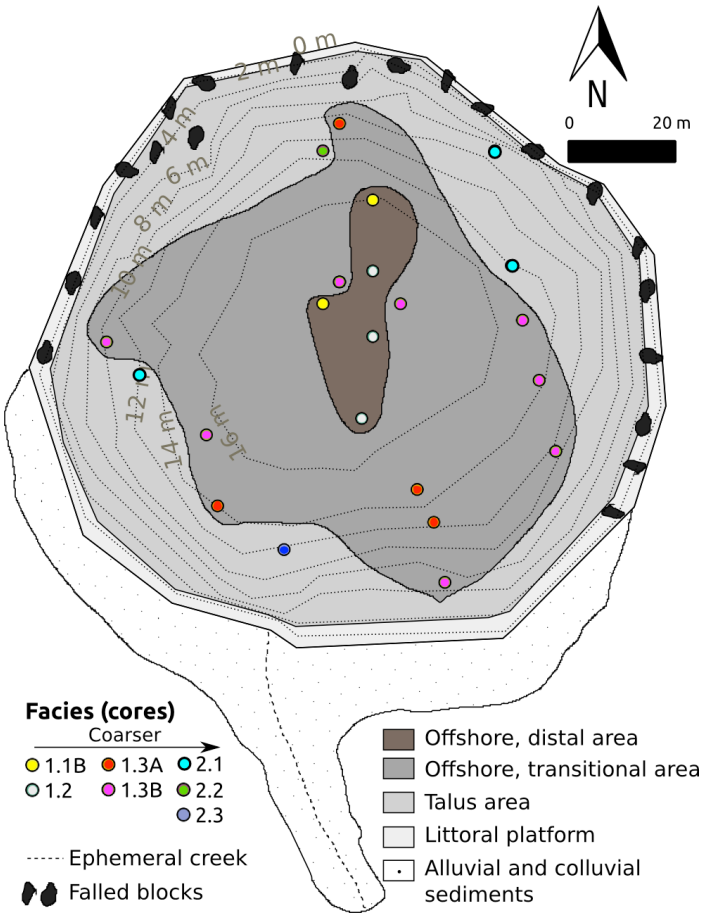

Fig. 9: Modern depositional sub-environments identified in lake La Parra.

max. length) characterized by black, massive fine-grained (facies 1.1B) and medium (facies 1.2) silts, with abundant OM. Sediments are transported as suspended load to distal areas and away from the influence of coarse terrigenous particles input.

Lake basin topography, water depth and distance to shore appear to be the main factors controlling the distribution of present-day surface sediments in the lake. The distance to shore obviously controls grain-size, showing a decreasing trend towards the distal areas (Fig. 9). Organic matter content decreases towards the transitional area and it is a mixture of terrestrial, submerged macrophytes and algal material. Around the N shore of the lake, an important factor contributing to the input of sediments to the lake is the block-falling processes along the steep scarp of the sinkhole, formed by dolostones and limestones, which may develop mass-wasting processes.

Chronological model

To construct the age model of La Parra sequence, seven of the nine radiocarbon dates listed in Table I were used. Two radiocarbon dates were rejected because they are not coherent with the age model. The date Poz-37956 (307±26 cal. yr. BP) is too young for its stratigraphical location in the sequence, and this could be due to contamination with younger material; the date Poz-37960 (2033±85 cal. yr. BP) shows an age older than two dates from stratigraphically lower intervals, suggesting reworking processes. The age model has been constructed by lineal interpolation between the dates.

Table I: Radiocarbon dates on La Parra core analysed at the Poznan Radiocarbon Laboratory, Poland (Poz-)

Drive	Core Depth (cm)	Laboratoy code	^{14}C AMS age (BP)	Calibrated age (2σ) (cal. yr. BP)	Calibrated age (2σ) (cal. yr. AD)	Material	Calibration
1	66	Poz-37954	230±30	291±24	1659 ±27	Wood fragment	INTCAL09
1	93	Poz-37955	390±35	468±43	1482 ±43	Wood fragment	INTCAL09
2	*145*	*Poz-37956*	*265±30*	*307±26*	*1644±26*	*Wood fragment*	*INTCAL09*
3	324	Poz-37957	1190±30	1117±64	834±64	Wood fragment	INTCAL09
3	375	Poz-37958	1155±30	1097±54	854 ±54	Wood fragment	INTCAL09
3	542.5	Poz-37960	1640±30	1548±66	403±66	Wood fragment	INTCAL09
4	*563*	*Poz-37960*	*1640±30*	*2033±85*	*-83±85*	*Wood fragment*	*INTCAL09*
5	624	Poz-37962	1700±30	1588±50	362 ±50	Wood fragment	INTCAL09
5	675	Poz-37963	1740±30	1639±77	311 ±77	Wood fragment	INTCAL09

Samples in italics were discarded (reversals or stratigraphically inconsistent)

According with this chronological model, the sedimentary record spans from 1639±77 cal. yr. BP (coinciding with the end of the Humid Iberian-Roman Period) to present (Fig. 8). The occurrence of 137Cs in the upper centimetre demonstrates that the sequence contains the sediments deposited during the last decades. The average sedimentation rate is 0,40 cm/yr but there are some changes along the sequence. The base of the sequence displays the highest sedimentation rate (1,46 cm/yr, Unit III) during a relatively

short period (around a century). During most of the sequence, sedimentation rate is about 0,36 cm/yr (Unit II and almost all the Unit I), corresponding to deposition of fine facies. The top sequence composed mainly of silts displays even lower (0,15 cm/yr) sedimentation rates.

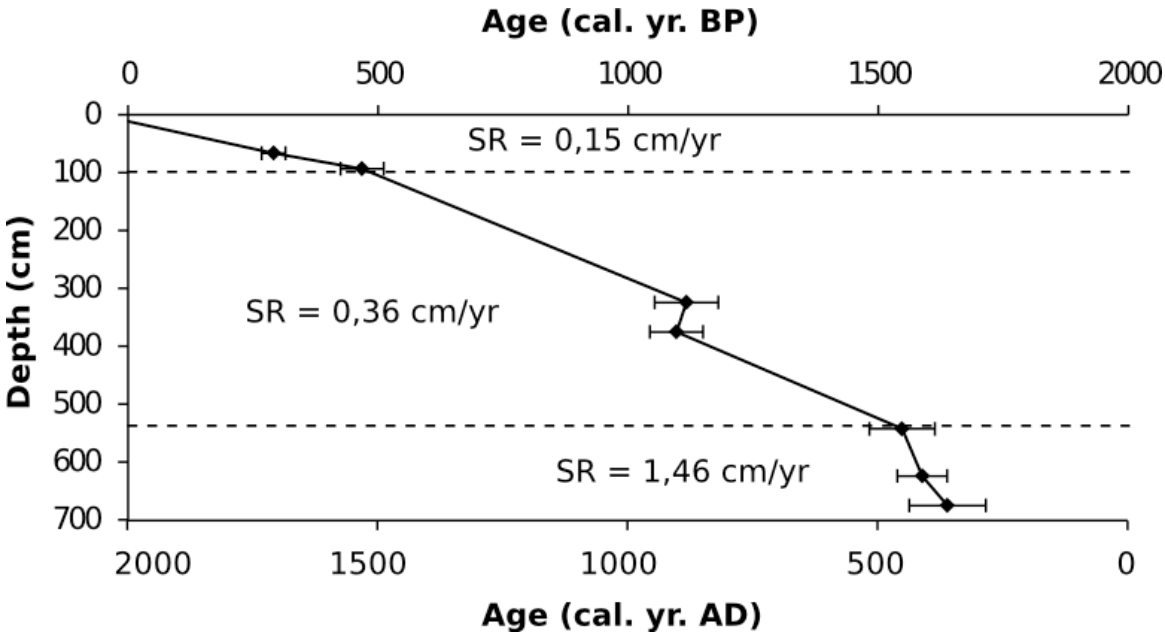

Fig. 8: Age model of the sedimentary record of lake La Parra constructed by lineal interpolation of seven radiocarbon dates.

Sedimentary Facies Analyses

The identification and interpretation of the different facies of the sedimentary record integrates the sedimentological and microscopical observations with geochemical data. The 6.95 m long core PA10-1A-U from the deepest part (17,5 m) of lake La Parra is mainly composed of carbonatic clastic sediments with variable amounts of organic remains. Eleven sedimentary facies and sub-facies have been identified and distributed in two main groups: i) clastic and ii) finely laminated with endogenic carbonate (Table II).

Table II: Description and interpretation of main sedimentary facies

Lithology	Facies	Description	Processes
	CLASTIC FACIES		
Silts	**1.1A** ***Fine grey silts***	Dark grey and massive, in beds of 10-25 cm and diffuse contacts, with abundant diatoms and amorphous OM. Abundant carbonatic and quartz grains.	Distal, relatively deep environments, more frequent anoxic conditions
	1.1B ***Fine black silts***	Massive, in isolated levels of 2-5 cm with net boundaries, with diatoms and amorphous OM. Abundant carbonatic and quartz grains.	
	1.2 ***Medium brown silts***	Dark and light banded, in layers of 5-20 cm with diffuse boundaries and macrophytes remains. Abundant carbonatic and angular quartz grains.	Distal to transitional setting; strong alluvial influence; rapid oxidation-reduction changes
	1.3A ***Coarse light silts***	Fining-upwards beds, 5-15 cm thick, with irregular basal boundaries. Disperse carbonatic cm-pebbles. Abundant mm-sized, OM fragments and presence of ostracods.	Turbidite - like processes, allochthonous material supply reaching the centre of the lake, moderate depth
	1.3B ***Coarse dark silts***	Beds of 2-10 cm thick, with irregular basal boundaries. They present abundant mm-sized OM fragments.	
Sands	**2.1** ***Fine green sands***	Massive, isolated levels of 3-4 cm in a green silty matrix. Dominated by angular carbonatic and quartz grains.	Littoral to transitional settings. High energy, relatively lower lake levels.
	2.2 ***Medium brown sands***	Massive, in levels of 2-10 cm with irregular boundaries with a silty fine-medium matrix. Abundant alotriomorphous and altered carbonatic grains.	
	2.3 ***Coarse brown sands***	A 10 cm thick, massive bed, with angular carbonatic pebbles and diatom fragments and irregular boundaries. .	
Gravels	**3.1** ***Fine brown gravels***	A 2 cm bed, massive, with irregular boundaries composed of carbonate pebbles and some invertebrate exoskeleton fragments.	Strong alluvial influence in a littoral setting. High allochthonous clastic input, and high energy
	3.2 ***Medium brown gravels***	A 30 cm thick bed, massive, with irregular boundaries. Pebbles are carbonatic, in a silty matrix.	
	LAMINATED, ENDOGENIC CARBONATE FACIES		
Silts	**4** ***Fine laminated silts***	Sets of 5 cm thick intervals with 1 mm thick white calcitic and dark OM-rich laminae with net and regular boundaries. Organic layer shows a high amount of diatoms and calcite layer is composed of homometric sub idiomorphous calcite grains.	Distal, low energy, frequently anoxic bottom waters; carbonate bioproduction, deep lake

Clastic facies

The following clastic facies have been identified (Fig. 10)

- **(1) Silts:** Intercalation between:
  - (1.1A) Fine grey silts: Dark grey massive silts, in beds of 10-25 cm with diffuse contacts. They are composed of heterometric carbonatic grains of 4-20 μm,, amorphous organic matter (OM) remains, diatoms and quartz grains of up to 80 μm.

  - (1.1B) Fine black silts: Black massive silts appear in isolated levels of 2-5 cm with net boundaries. They are composed by heterometric carbonatic grains of 4-12 μm with abundant amorphous OM, macrophytes fragments and homometric grains of quartz of up to 25 μm.

  - (1.2) Medium brown silts: Weakly-banded silts formed by 2 cm thick dark and brown layers, appearing in beds of 5-20 cm with diffuse boundaries. They are form by homometric and irregular carbonatic grains of 10-20 μm, with homometric quartz grains of 20-50 μm, and macrophytes fragments.

  - (1.3A) Coarse light silts: Brown beds, 5-15 cm thick, with fining-upwards textures and, irregular basal boundaries. They present disperse carbonatic grains of less than 2 mm, with abundant OM fragments. Microscopically, they are composed by heterometric carbonatic grains with two main distributions: i) fine, 4-10 μm and ii) coarse, less abundant, of 50-60 μm; also there are abundant remains of amorphous OM and some ostracods, and homometric sub-angular quartz grains of 50-100 μm.

  - 1.3B) Coarse dark silts: Dark brown, 2-10 cm thick beds with irregular basal boundaries. They present abundant mm macrophyte fragments. Microscopically, they are composed by heterometric carbonatic grains with two main groups: i) fine, more abundant, average 10 μm and ii) coarse, sub-angular grains, of 50-70 μm; also there are abundant remains of macrophytes and amorphous OM and homometric quartz grains of 25-50 μm.

Sedimentological features of facies 1.1A and 1.1B indicate low energy transport processes linked to deposition of fine particles near the centre of the lake, away from the influence of coarse terrigenous alluvial input and presumably with relative high lake levels. Bottom conditions would fluctuate between more oxic conditions (grey silts) and more reduced ones (black silts).

The occurrence of abundant rounded, irregular calcite grains and abundant macrophyte fragments in Facies 1.2 suggests dominant traction transport processes. Alternation of brown and dark layers also implies relative rapid changes in oxidation/reduction conditions.

Coarse silt facies (1.3A and 1.3B) present normal gradation and irregular basal boundaries, suggesting turbidite - like processes carrying allochthonous material to the centre of the lake.

- **(2) Sands:**
  - (2.1) Fine green sands: Massive, isolated levels of 3-4 cm composed of a green silty matrix, and heterometric, angular carbonatic grains of 4-100 μm and quartz of 20-100 μm, with abundant amorphous OM and macrophytes remains.

  - (2.2) Medium brown sands: Massive, in levels of 2-10 cm with irregular

boundaries. They are composed of a fine-medium silty matrix and homometric alotriomorphous-altered carbonatic grains of 4-10 μm, with amorphous OM, macrophytes remains, invertebrate exoskeletons and heterometric angular quartz grains of 50-100 μm.

- (2.3) Coarse brown sands: Massive, with angular carbonatic pebbles of about 1 mm, and some up to 1 cm, in a level of 10 cm with very irregular boundaries. The matrix is composed by medium silt with heterometric angular, carbonatic grains, amorphous OM, diatoms remains and homometric angular quartz grains of 20-100 μm.

Sand facies represents littoral to transitional deposition from relatively low energy (fine sands) to high (coarse sands). They represent alluvial input of watershed sediments and littoral erosion of previously deposited lake sediments transported to deeper areas of the lake.

- **(3) Gravels:**
  - (3.1) Fine brown gravels: Massive, in only one bed, 2 cm thick with irregular boundaries. Pebbles are carbonatic in composition, heterometric (less than < 5 cm) and angular. The matrix is formed by fine silts, with heterometric carbonatic grains of 10-40 μm and homometric quartz grains up to 40 μm. Amorphous OM and diatoms remains are also present.

  - (3.2) Medium brown gravels: Massive, in only one bed 30 cm thick, with very irregular boundaries. Pebbles are carbonatic, less than 5 cm long, in a silty matrix. Matrix is composed by heterometric alotriomorphous carbonatic grains of 4-25 μm. Diatoms, amorphous OM, invertebrate exoskeleton fragments and heterometric quartz grains of less than 100 μm are also present.

Gravel facies imply very high-energy traction transport of allochthonous sediment originated in the watershed and transported by the small creek located at the SW of the lake and also reworking of sediments from shallow zones around the lake. Deposition of these facies in the centre of the lake suggests littoral environments dominated even these areas.

Laminated, endogenic carbonate facies

There is only one facies in this group (Fig. 10):

- **(4) Fine laminated silts with endogenic carbonate:** Constituted by 5 cm thick intervals composed of 1 mm thick white calcitic and dark OM laminae with net and regular boundaries. Calcite layers are composed by homometric sub-idiomorphous carbonatic grains with some amorphous OM and homometric angular quartz grain of up to 30 μm. Diatoms are very abundant in this facies, particularly in the organic laminae.

The distinctive characteristic of facies 4 is the presence of laminations and the occurrence of endogenic calcite. It consists of couplets of light (white) and dark (black) laminae, similar to carbonate laminites found in many karstic lakes in Spain (Zoñar, Martín – Puertas et al., 2008; Arreo, Corella et al., 2010; Montcortès, Corella et al., 2010; La Cruz, Romero-Viana et al., 2008). The light laminae are composed of calcium carbonate

crystals formed in the epilimnion during algae blooms in summer and the dark ones consist mainly of organic-rich silts with some fine quartz clasts deposited during late summer and winter.

Laminations in lacustrine deposits are frequently associated with a lower energy environment, less alluvial influence, and the existence of stratified waters, usually in deeper lake level stages (Brauer et al., 2004).

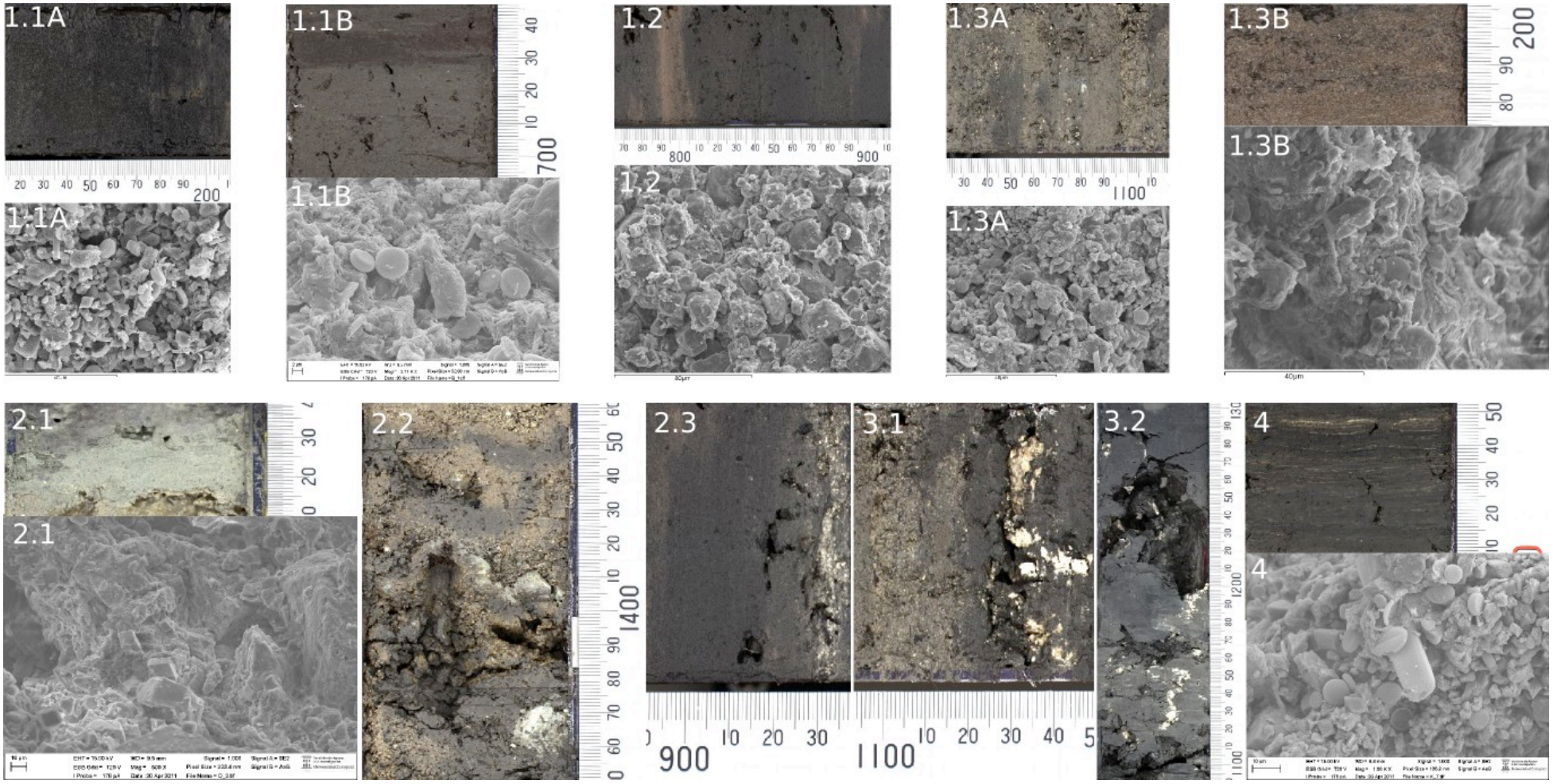

Fig. 10: 1.1A) Fine grey silts - SEM image: homometric calcite and diatoms. 1.1B) Fine black silts - SEM image: altered crystals of dolomite, round quartz grains and diatoms.1.2) Medium brown silts - SEM image: rounded and irregular carbonatic grains.1.3A) Coarse light silts - SEM image: heterometric irregular dolomite grains. 1.3B) Coarse dark silts - SEM image with heterometric dolomite grains. 2.1) Fine green sands with the characteristic green matrix. 2.2) Medium brown sands showing some of the light carbonatic pebbles. 2.3) Coarse brown sands and finer silty facies.3.1) Fine brown gravels whit white carbonatic pebbles. 3.2) Medium brown gravels. 4) Fine laminated silts - SEM image: abundant diatoms and fine endogenic calcite crystals

Substrate

The base of La Parra lacustrine sequence is the Cenomanian green marl formation. The substrate consists of gravels (Fig. 11) with a green matrix and some evidences of chemical alteration (corrosion, dissolution) of the heterometric and angular carbonatic pebbles (0,5-5 cm). The matrix is formed by homometric angular carbonatic grains of 50-70 µm and quartz of 80-100 µm.

Litostratigraphic Units.

The sedimentological and geochemical analyses (see text below) allowed to distinguish three main lithoestratigraphic units (units I to III, Fig. 12) corresponding to the

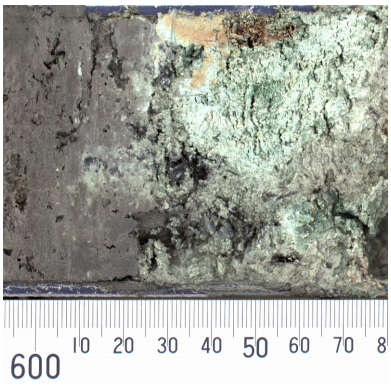

Fig. 11: Photograph showing the base of the sequence: altered green Cenomanian marls.

lacustrine record. The base of the sequence (Unit IV) is composed of Cenomanian green marls, with evidences of karstic alteration (dissolution and brechification textures).

Unit III is formed by a coarsening upward sequence, showing medium brown silts (facies 1.2) in the bottom and an alternation between coarse dark silts (facies 1.3B) and fine green sands (facies 2.1) towards the top.

Unit II presents a fining upward sequence, which starts with fine and medium brown sands (facies 2.2), followed by an alternation between coarse black silts (facies 1.3B) and medium brown silts (facies 1.2) distributed in layers from 5 to 20 cm thick.

Unit I is composed of three fining upward sequences: i) the lower,

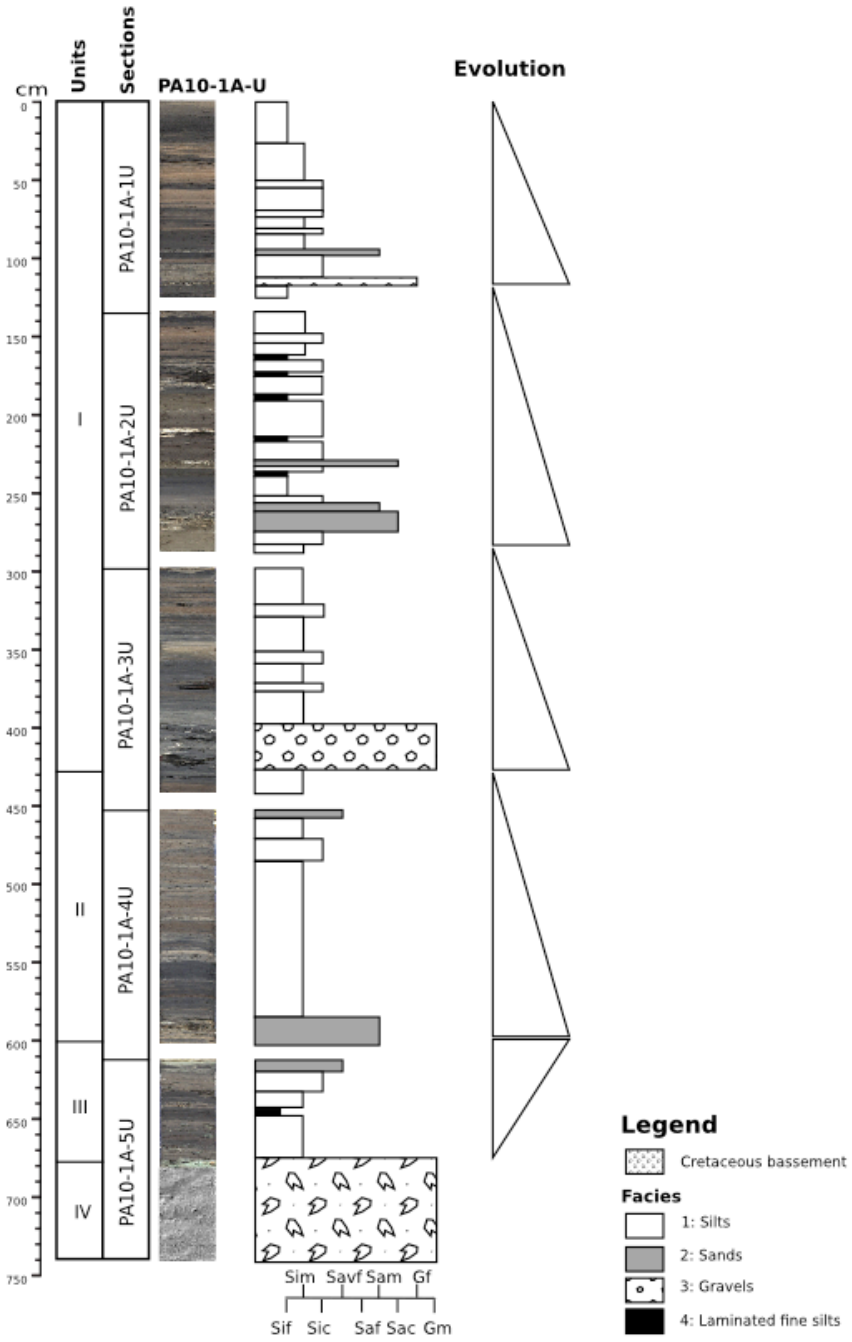

Fig. 12: Sedimentary sequence for PA10-1A-U core, including: sedimentary units and sections, core CCD image, sedimentological profile and grain evolution of main sequences. Sif: fine silts; Sim; medium silts, Sic, coarse silts; Savf: very fin sands; Saf: fine sands; Sam: medium sands; Sac: coarse sands; Gf: fine gravels; Gm: medium gravels.

formed by a 30 cm interval of medium brown gravels (facies 3.2), followed by alternating coarse black silts (facies 1.3B) and medium brown silts (facies 1.2) in layers of 10-15 cm thick; ii) the intermediate sequence is the most variable in facies; it starts with a fining upward 40 cm thick subsequence, from coarse brown sands (facies 2.3) to fine laminated silts (facies 4), and continues with an alternation of coarse dark silts (facies 1.3B) and fine laminated silts (facies 4) -with presence of facies 1.3A and 1.2-; towards the top, coarse black silts (facies 1.3B) and medium brown silts (facies 1.2) with facies 4 occurs; iii) the upper sequence is formed by two fining upward subsequences: the lower one, 20 cm thick, is composed by fine brown gravels (facies 3.1), coarse light an dark silts (facies 1.3A and 1.3B) and medium brown silts (facies 1.2), and the upper subsequence, 95 cm thick, starts with medium brown sands (facies 2.2), continues with alternating facies 1.3B and1.2, and finishes with fine grey silts (facies 1.1A).

Mineralogy

The sediments of lake La Parra are mainly composed of three mineral types (Fig. 13): *carbonates*, the most important contributors (91,4 %), with dolomite, calcite, magnesian-calcite and aragonite; *clay minerals* (5,1 %) represented by illite and clinochlore; and other *silicates* (3,5 %), mainly quartz and microcline. The mineralogy is dominated by dolomite, which is coherent with the carbonated steep scarps (basically dolostones) surrounding the lake's basin and the watershed.

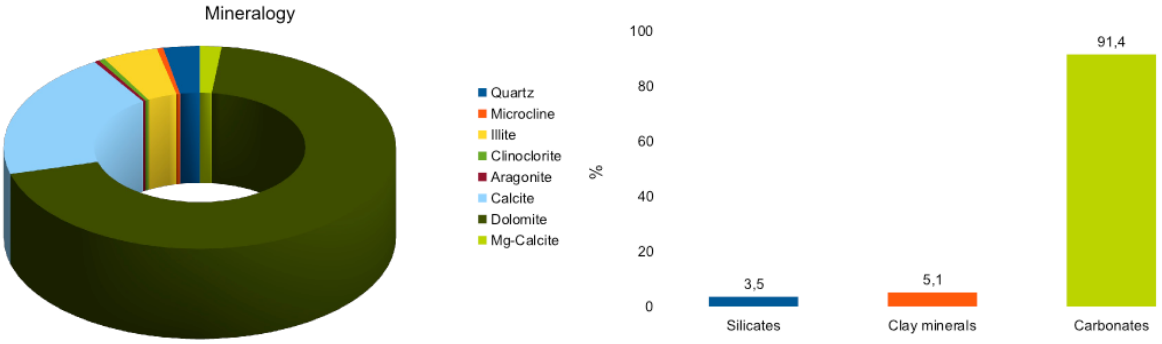

Fig. 13: Left: Average distribution of different minerals measured by X-ray diffraction (XRD) for the sedimentary record of Lake La Parra in percentages. Right: Percentages of the mineralogical species grouped by families.

In Fig. 14 the mineralogical composition of Lake La Parra sediments are represented versus the composite depth. Mineralogical composition does not show large changes through the sequence. Nevertheless based on mineral dominance and the occurrence of some minor mineral phases, the three sedimentological units show some differences.

Unit III is characterized by high values of dolomite, illite and quartz, decreasing towards the top, and the presence of aragonite, calcite and Mg-rich calcite in some intervals..

Unit II and the bottom of Unit I are characterized as well by high values of dolomite, illite and quartz. These minerals experiment a slight decrease at the beginning of Unit I, coinciding with the deposition of gravels. During Unit II, Illite and clinochlore present high values, coherent with the abundance in fine-grained facies.

The middle of Unit I is characterized by the highest values in calcite, and the occurrence of Mg-calcite and aragonite. Aragonite occurs in two intervals at the onset of deposition of laminated facies and just after them. During deposition of laminated facies, clinochlore and illite are more abundant.

The top of Unit I is characterized by higher calcite and illite contents and the decrease of dolomite.

One of the clear features of the mineralogical composition of La Parra sequence is that silicate fraction (quartz, clay minerals, microcline) distribution presents a similar pattern as dolomite. That is a clear indication of the clastic nature of dolomite in La Parra Lake. This assessment is supported by the fact that well-formed, euhedral dolomite crystals have not been identified, either on sediment frotis or SEM images in any facies. The illite and clinochlore are more abundant in fine-grained facies.

Calcite has an opposite pattern compared to dolomite, showing significant peaks in Unit III and in the middle of Unit I. The peak of Unit III and the peaks of Unit I coincide with the presence of aragonite (580, 240 and 120 cm respectively), and they are related to laminated facies. Mg-calcite, occurs at the transition between Unit III and II and in the middle of unit I, and it seems associated to shallowing – upwards trends from silts to sands. It is interesting to notice that Mg-Ca peaks always occur prior to aragonite peaks, suggesting that carbonate phase succession could be related to increase salinity as shown in other carbonate lakes (Morellón et al., 2009).

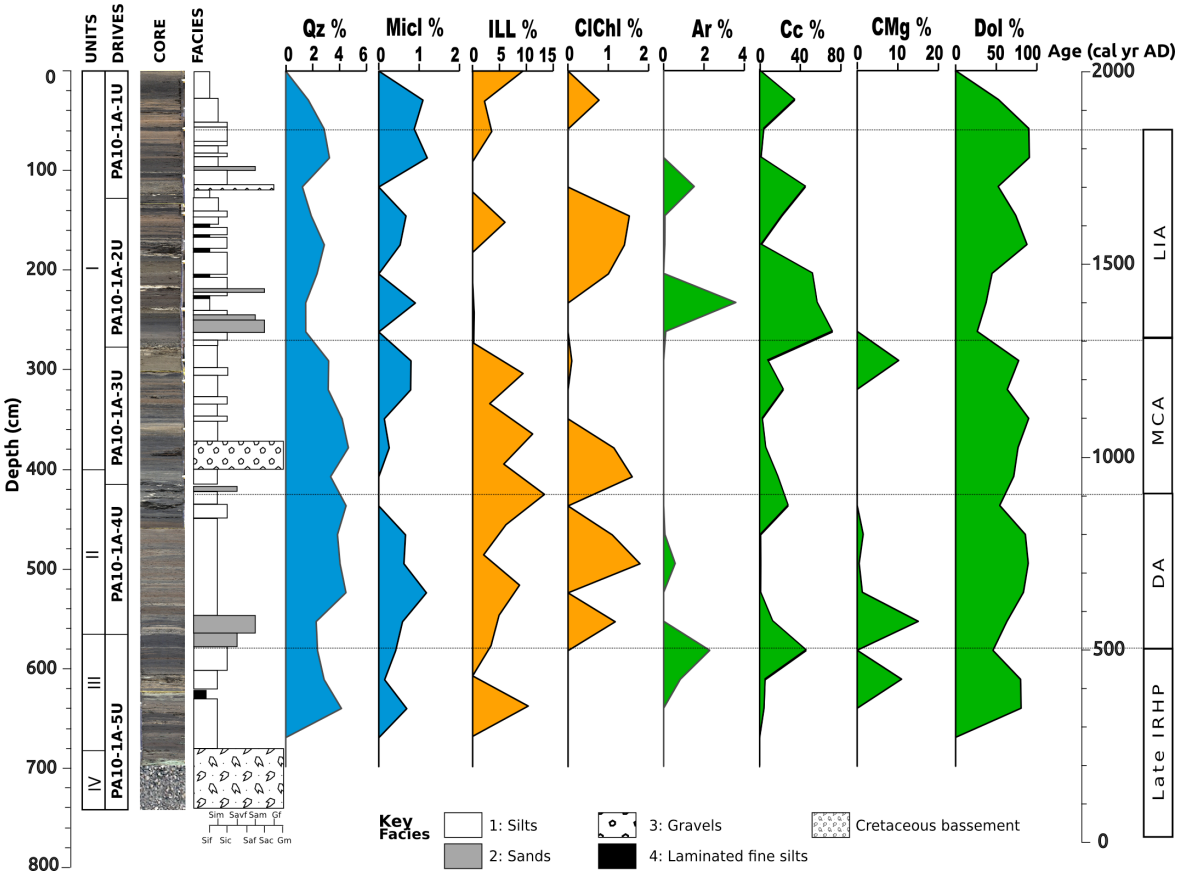

Fig. 14: Mineralogical profiles measured by X-ray diffraction (XRD) for the composite sequence of Lake La Parra in percentages versus depth. Lithological units are indicated by the left panel.

Geochemistry

XRF analyses allow high-resolution reconstructions of past global and climate changes in marine sediments (Richter et al. 2006) and in lakes (Moreno et al., 2008; Saez et al., 2009). It has been found that the relationships between the intensity of the XRF signal between different elements vary over time with changes in lake dynamics, which is ultimately driven, by changes in climate or in the lake environment or the watershed (Kylander et al., 2011). Several examples of karstic lakes in Spain have been recently

published – Laguna Zoñar, Martín–Puertas et al., 2008; Laguna Taravilla (Moreno et al., 2008), Laguna Estanya (Morellón et al., 2008), Lago Arreo (Corella et al., 2011; Lago Montortès, Corella et al., 2011; – highlighting the potential of this technique in small, karstic lakes.

X-ray fluorescence analyses need core samples with a flat and smooth surface. The water content generally ranges from 80 to 30% in the uppermost centimetres of lake sediments (Fig. 15), with a rapid decrease immediately below the sediment surface. Effects of sample inhomogeneity and surface roughness are particularly pronounced for sediments containing abundant medium-coarse sand-sized particles such as shell fragments, coarse pebbles in finer matrix, macrophytes fragments, etc., but are less significant in most fine-grained homogeneous sediments. Sample preparation includes (Richter et al. 2006) *careful* flattening of the sediment surface to remove irregularities from core slicing. The sediment surface is subsequently covered with thin (4 µm) Ultralene ® film, further diminishing surface roughness and preventing contamination of the prism unit during core logging.

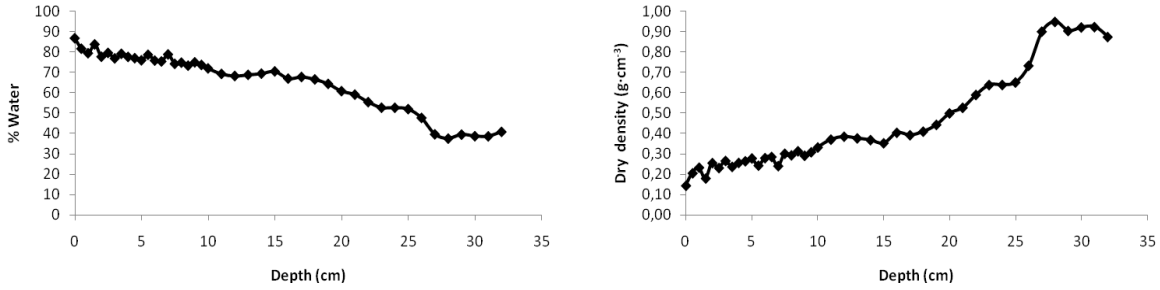

Fig. 15: % Water content (left) and dry density (right) versus depth in the parallel short-core PA-10-2A-1G34 (34 cm length, centre of the lake); both related with the porosity of sediments.

It is important to remark that variations of physical properties such as grain size or porosity affect (Fig. 15) the amount of scatter radiation at the surface of the sediment sample and, hence, the amount of radiation received by the sample; consequently the total element intensities, calculated as the sum of all element intensities, decline with increasing grain-sizes (Tjallingii, 2006). Decreasing of total intensities with increasing grain size is probably related with increasing radiation scatter on rougher sediment surfaces of coarse-grained sample material. The poor quality of samples used for XRF logging, compared to fused beads or powder pellets of known density of conventional laboratory X-ray fluorescence, necessarily means that XRF logging data are only semi-quantitative, and the results are always expressed as counts per second (cps). However XRF logging records faithfully trace relative down-core variations in the elemental composition of sediments.

In lake La Parra, the XRF has helped to understand better some lake processes, as clastic input, carbonate deposition, organic productivity, evolution of redox stages at the bottom of the lake and the human impact in the watersheds.

Correlation analyses and relation between elements

To understand better the relation between the main elements analyzed on the core PA10-1A-U (Ti, Al, K, Ca, Rb, Sr, Fe, Mn, Pb, Cu, Zn, Zr and Si) a basic correlation analysis has been performed (Table III).

Table III: Correlation coefficients among the elements obtained by the Avaatech XRF Core Scanner

	Si	Ca	Ti	Mn	Fe	Rb	Sr	Zr	K	Al	Pb	Cu	Zn
Si	1,00												
Ca	0,87	1,00											
Ti	0,93	0,76	1,00										
Mn	0,79	0,68	0,92	1,00									
Fe	0,88	0,72	0,98	0,91	1,00								
Rb	0,53	*0,21*	0,64	*0,49*	0,64	1,00							
Sr	*0,20*	*0,27*	*0,17*	*0,13*	*0,15*	*0,16*	1,00						
Zr	*0,45*	*0,20*	0,60	0,56	0,56	0,79	*0,07*	1,00					
K	0,97	0,82	0,97	0,83	0,95	0,63	*0,19*	0,52	1,00				
Al	0,99	0,81	0,89	0,73	0,84	0,54	*0,19*	*0,45*	0,92	1,00			
Pb	*0,22*	*0,03*	*0,32*	*0,29*	*0,32*	*0,43*	*-0,07*	*0,45*	*0,24*	*0,21*	1,00		
Cu	*0,14*	*0,10*	*0,15*	*0,14*	*0,15*	*0,12*	*-0,01*	*0,08*	*0,11*	*0,13*	*0,20*	1,00	
Zn	*0,47*	*0,19*	0,57	*0,48*	0,55	0,75	*0,04*	0,70	*0,46*	*0,47*	0,54	*0,24*	1,00

Values in italics are below 0.5 suggesting a low correlation among the elements

According to these correlations, two groups can be identified: i) Si, Al, Ti, Fe, Ca, K and Mn; and ii) Zr, Rb and Zn, suggesting a similar origin for these elements. Sr, Pb and Cu are the only elements that do not show any correlation with the others, indicating a different source for these elements, likely related to autochthonous bio-production (Sr) (Kylander et al., 2011) and human impact in the watershed (Pb and Cu).

The relative variations of these elements along the core (Fig. 16 up), are coherent with the three main lithological units: i) Unit III is characterized by medium-low signal intensities in Ti, Al, Si, Mn, Fe and Ca elements; ii) Unit II presents the highest counts per second of the sequence in all elements with exception of Cu and Sr; iii) Unit I has the lowest intensity values in Ti, Al, Si, Mn, Fe and Ca, presenting lower values in the rest of elements with exception of Sr, which shows the highest counts per second.

Since the mineralogical analyses do not shows relevant changes in composition along the whole sedimentary record, the exceptional increase in XRF signal intensity along Unit II of most analyzed elements can be interpreted as a response to variations in physical properties of sediments. This unit is mainly composed by relatively homogeneous fine facies (silts) with lower porosity compared to relatively more inhomogeneous composition of Units I and III, including fine laminated to gravels facies.

To better interpret the relative changes in XRF intensities for different elements, a previous normalization is needed. Assuming titanium as an allochthonous element, indicative of exogenous input to the lake, it has been used to normalize the rest of the elements.

When using the normalized data (Fig. 16), the element intensities show three main intervals, coherent with the lithological units. The main changes in geochemical composition of the sediments took place at the beginning of the Medieval period, the Dark Ages (DA, 500-900 AD) (cm 580), during the Medieval Climate Anomaly (MCA, 900-1300 AD) (cm 425) and finally during the Little Ice Age (LIA, 1300-1850 AD) (cm 265).

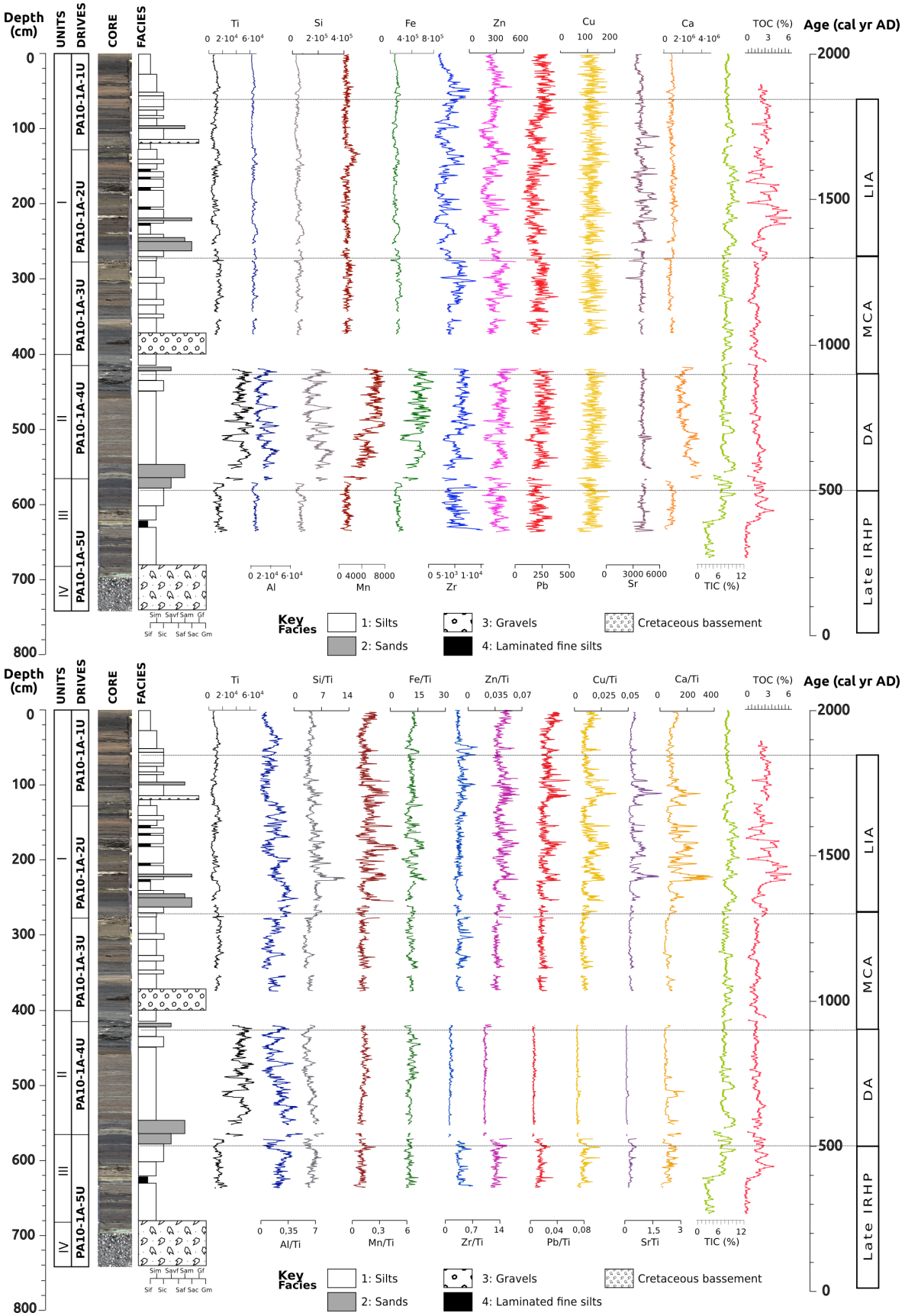

Fig. 16: Up: Ti, Al, Si, Mn, Fe, Zr, Zn, Pb, Cu, Sr, Ca ratios vs. depth and calibrated ages AD profiles, as well as TIC and TOC. Down: Same graphic showing the elements normalized by Ti..

From a geochemical point of view, the La Parra core can be subdivided in three sections. From 640 to 560 cm, in pre-MCA times, elements present higher intensities than during the MCA, as is the case of Zr, Zn, Pb, Cu, Sr and Ca. From 560 to 265 cm, during the MCA, a sharp decrease in the signal of these elements occur, showing smooth and very low amplitude changes in all of them with the exception of Al and Si. From 265 to 80 cm, all the elements, with exception of Al, present their highest values, showing two important peaks during the LIA, at 220 and 110 cm. At 75 cm, peaks in Mn, Fe, Zr, Zn, Pb, Cu and Sr mark the end of the relative high values of the LIA.

Ti, Al, Si and Zr are all indicative of minerogenic, clastic input to the lake (Kylander et al., 2011). In Lake La Parra these elements generally show the same trends across the suite with some differences in signal between Al/Ti, Si/Ti and Zr/Ti (Fig. 16): relatively high values during pre-Medieval times, a sharp decrease during the Dark Ages and a very slight increase at the end of the medieval epoch (MCA). During the LIA, these elements present relatively high values but with a progressive decreasing trend until the end of this period (cm 80), which is maintained up to recent times.

These geochemical profiles suggest a relatively high allochthonous input to the lake during the Late Iberian-Roman Humid Period, (IRHP, 300 - 550 AD) followed by a dramatic decrease during the Dark Ages with the sedimentation of fine facies (Unit II). During the end of the MCA a new increase in clastic material to the lake occurred, followed by a slight decrease during the LIA. During the last century, a sharp decrease is indicated by Al/Ti and Zr/Ti ratios, while Si/Ti maintains relatively low values as before.

Regarding to carbonate deposition, Ca and Sr in lake sediments are related to both, carbonate input from the catchment and in-lake precipitation of different phases of $CaCO_3$ when chemical concentration of lake waters reaches the point of carbonate saturation, during low lake levels phases or biological processes (Cohen, 2003).

The Lake La Parra bedrock is dominated by dolostones and limestones, providing a large pool of carbonates to draw from. The carbonatic component is dominant in the detrital sediment contribution. At same time, deposition of carbonates induced by biological activity has been described in these karstic lakes during the spring–summer bloom of phytoplankton (Julià et al., 1998; Rodrigo et al., 2001; Romero et al., 2006; Romero-Viana et al., 2009).

Figure 16, shows the Ti normalised profiles of Sr, Ca and Si as well as the related proxies of total organic (TOC) and total inorganic carbon (TIC). The Ca profile is similar to the Ti one, except during some intervals in Unit II, with a marked peak in cm 510. Sr/Ti profile is similar to Ca/Ti and both show the highest values during the LIA, where two important peaks in 220 and 110 cm, coinciding with the deposition of sands and fine gravels respectively. TIC profile shows little variability during the whole sedimentary record, showing the lowest values during the onset of lacustrine sedimentation (IRHP period). The TOC profile is similar to the TIC one, but differs during the LIA period, showing its highest values coinciding with the sedimentation of discrete 2-5 cm fine laminated, facies with endogenic calcite, and it most important peak coincides with the Sr/Ti and Ca/Ti peak of cm 220. Calcite sedimentation peaks during the LIA, when clastic inputs where smaller.

Manganese has been used as an indicator of the evolution of redox stages in the bottom of the lakes, because, manganese forms a highly insoluble oxide in an oxygen-rich environment and migrates up to the oxic boundary. Changes in lake oxygen levels can be the result of changes in lake levels and ventilation of the water column or increased biological activity (photosynthesis) (Kylander et al., 2011).

Fe and Mn show a high correlation coefficient with clastic-related elements proxies as Ti and Si, but Mn presents a inverse relationship in Units III and II (Fig. 16), which could be interpreted as a period with relatively lower oxygenation of waters, probably with high lake levels. The high Mn/Ti peak at the end of Unit III, coinciding whit a decrease of Si/Ti

may reflect changes in biological activity. Mn precipitation could be a sign of oxygenation of the bottom waters through an increase in productivity or by lowering of lake levels as seen, for example, in the Lago Chungará sequence (Moreno et al., 2007). Although an important role for increased bioproductivity is further supported by relatively high peaks in Ca/Ti and Sr/Ti and TOC, the presence of coarser facies (sands), also points to short periods of lower lake levels. During Unit I and the beginning of the LIA, Mn follows a trend similar to clastic proxies, and it increases with a general increase in sediment input rather than with a decrease in oxygenation of the water column. Nevertheless, the highest values of Mn/Ti coincide with the period of laminated anoxic facies sedimentation, suggesting high lake levels during the LIA.

Heavy-metals as Pb, Cu and Zn have been interpreted as a sign of anthropic influence in lakes and watersheds. These elements do not present any significant correlation with others and if normalised by Ti (interpreted as detritic proxy) (figure 16, bottom), they show very low values and similar trends. They have a relatively high peak at the end of Unit III (590 cm), very low values during Unit II and they show the highest values in the more recent sediments of mid-top Unit I, with high peaks in 180, 120 and 10 cm. These profiles are similar to the ones related to clastic proxies (see Fig. 16, bottom). This similar pattern and their low values suggests that they correspond with the trace elements or impurities taking part on the mineral structure of main detritic-weather resistant minerals rather than with human impact.

Discussion

Depositional history and sedimentary environments during the last 1600 years

Based on facies associations (Table II) and geochemical analysis (Fig. 16 XRF elements), five main stages can be inferred for the evolution of Lake La Parra during the last 1600 yr (Fig. 17).

Stage I: The onset of lacustrine sedimentation with a rapid increase in water table levels and development of anoxia in the bottom of the lake (300 – 500 cal. yr AD)

The karstification processes and collapse that created the La Parra sinkhole occurred during the Pliocene Main Erosion Phase in the Iberian Chain (Alonso, 1986). The La Parra basin had been a dry Torca with the phreatic level under the topographic surface during most of the Quaternary, and it was only flooded at about 300 cal yr. AD, as the available radiocarbon dates indicate. It was during the late Iberian-Roman Humid Period (IRHP, 300-500 cal. yr AD), when lacustrine sedimentation started characterized by a rapid increase of detrital input (Unit III, sedimentation rate of 1,46 cm/yr). The sedimentation of fine laminated facies (facies 4) suggests a rapid evolution towards relatively deep environments, with increasing the lake levels until the development of reducing conditions in the bottom of the lake to permit the preservation of finely laminated facies.

Around 400 cal. yr AD, the deposition of a coarsening sequence (coarse silts to sands, facies 1.3 and 2.1 respectively) and the presence of aragonite and high-Mg calcite in the mineral fraction imply the dominance of more littoral environments in the lake and the development of more mineralized waters suggestive of a rapid drop of water table levels and the development of a shallow lake. This stage is characterized by rapid hydrologic changes with littoral and relatively deep depositional environments alternating.

Stage II: A shallow to deep lake between 500 - 900 cal. yr AD

This stage coincides chronologically with the Darks Ages (DA, 500 - 900 cal. yr AD) and starts with deposition of coarse sand facies but decreasing clastic input as indicated by lower Si/Ti, Al/Ti, Zr/Ti ratios. The presence of a well-developed littoral vegetation belt and reduced run-off, could explain the lower clastic input during this period of relatively lower lake level.

The deposition during Unit II of homogenous medium-silt facies is interpreted as the increment of fine sediment delivery to the lake and a rapid increase of water table levels. Moreover, the dominance of fine facies and relatively high values of Al/Ti, Si/Ti and Fe/Ti suggest a high fine-sediment input (Kylander et al., 2011) due to the synergetic effects of changes in the hydrological system (higher lake levels), higher anthropic alteration of the environment (minor vegetal coverture, increase in erosion) and increase in run off due to higher rainfall.

Stage III: Lower lake levels and increase in detritic input from 900 to 1400 cal. yr AD

The onset of the Medieval Climate Anomaly (MCA, 900 cal. yr AD) in Lake La Parra is characterized by deposition of gravels, and increasing ratios of Al/Ti, Si/Ti and Ca/Ti. During this stage, coarser carbonatic facies with detrital OM are deposited. At the end of this episode (1300-1400 cal. yr AD), aragonite and high-Mg calcite are formed in La Parra, indicative of a high Mg/Ca ratio and a relatively high water salinity during a period with dominancy of littoral and shallow clastic facies and higher concentrated waters.

Stage IV: Highest lake levels and development of frequent anoxic from 1400 to 1850 cal. yr. AD

The dominance of fine facies during the intermediate subsequence of Unit I and specially the deposit of fine laminated facies 4 with endogenic calcite, and the high values

of Sr/Ti, Ca/Ti, TIC and TOC, single out a period from 1400 to 1700 cal. yr. AD with the highest lake levels and frequent anoxia in the bottom. During this period - chronologically coinciding with the Little Ice Age (LIA, 1300-1850) - the absence of high-Mg calcite in the mineral phases suggest less mineralized waters. Development of laminated facies, longer periods of meromixis and higher lake levels have been described as well in the nearby Lake La Cruz (Julià et al., 1998) during this period.

Two periods of relatively lower lake levels during this stage have been identified. A short dry period in the XVth century (1450-1400 AD) is suggested by the presence of coarser sandy facies and high values in Ca/Ti and Sr/Ti ratios.

Later on, coarse clastic facies are deposited around 1700 cal. yr. AD (facies 3.1 and 2.3), coinciding with high values of Sr/Ti, Ca/Ti, Pb/Ti, Cu/Ti and Zn/Ti, suggesting an increase in clastic inputs and relatively lower lake levels, probably due to a new agricultural period.

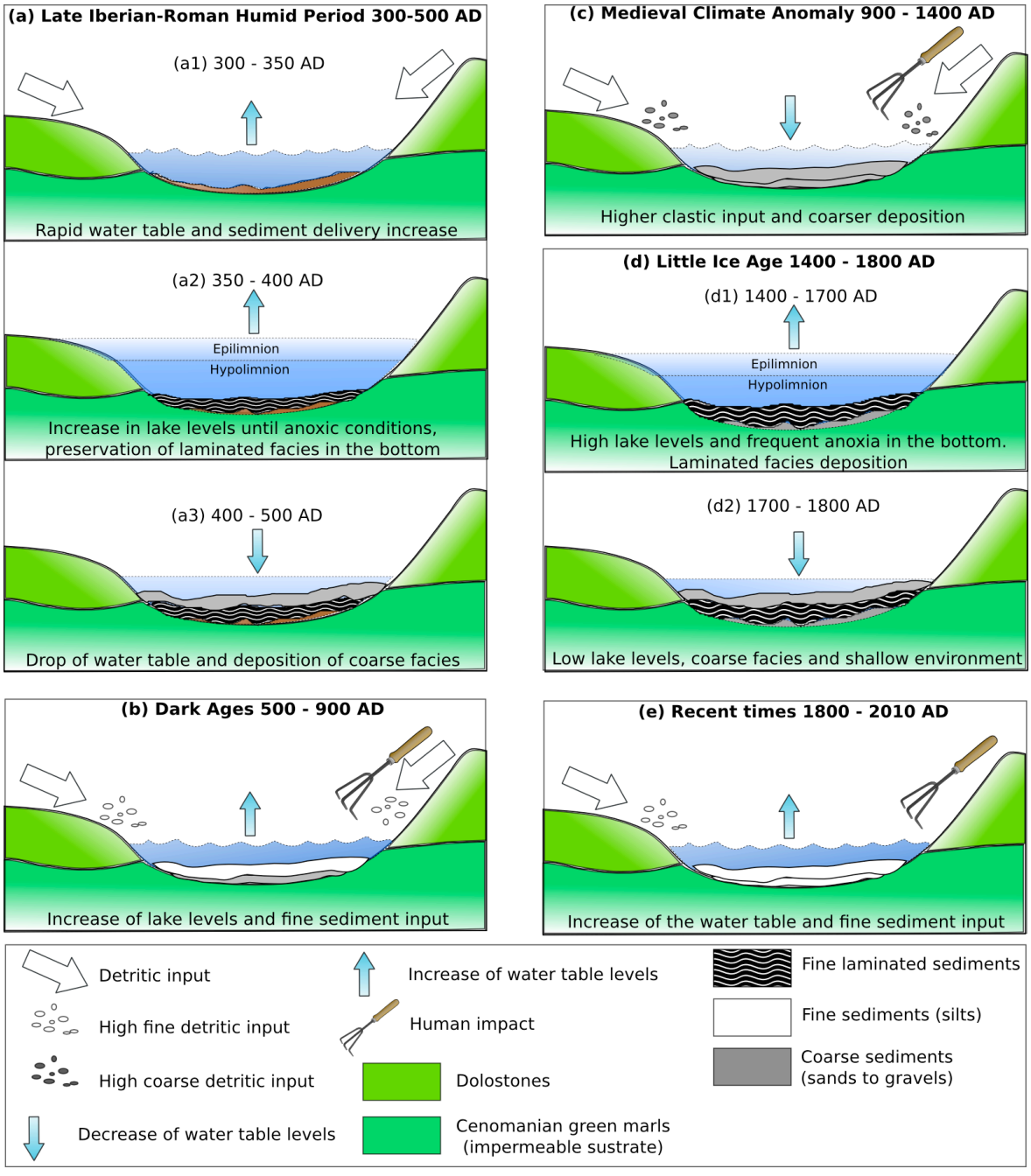

Fig. 17: The five main stages of the depositional history and environmental evolution of Lake La Parra during the last 1600 cal. Yr AD.

Stage V: Slight increase of lake levels on recent times, from 1850 to 2010 cal. yr. AD

The dominance of massive fine silts in the upper part of Unit I indicates a slight increase of water table levels on recent times, after 1900 AD, coinciding with a decrease in Al/Ti and Si/Ti ratios. Contrary, Pb/Ti, Cu/Ti and Zn/Ti show increasing values, maybe indicating a major human impact in the basin due to agricultural practices during the last century. The absence of fine laminated facies and the high values of Mn/Ti, suggest the dominance of oxic bottom conditions.

Climate and Human Impact in Las Torcas Complex during the last 1600 years

Climatic changes are expected to amplify the hydrological variability in the Mediterranean region, where climate, water availability and human activities have been strongly interdependent. The paleohydrological fluctuations and the evolution of the sedimentary environments in La Parra provides an excellent case study of such variability, because the sedimentary record of Lake La Parra is the longest and more accurately dated record of Las Torcas Complex, spanning the last 1600 cal. yr. BP. Other available paleohydrological reconstructions in this lake complex from La Cruz Lake and Lagunillo del Tejo sedimentary records, see figures 18 and 19 (Julià et al., 1998; Romero-Viana et al., 2010; López-Blanco et al., 2011), have also identified several climatic fluctuations during the last millennia, particularly the Medieval Climatic Anomaly (MCA) and the Little Ice Age (LIA), showing rapid successions between wet and dry periods.

Episode I: The onset of lacustrine sedimentation during the end of the Iberian-Roman Humid Period (IRHP), 300 to 500 cal. yr AD, with a rapid increase in water table levels and development of anoxia.

The rise in water level would have coincided with an increase in regional humidity, which have been observed as well in nearby lacustrine records (Lake El Tejo, unpublished data) and in other examples from the NE Spain as the lakes Estanya (Morellón et al., 2009) and Moncortés (Corella et al., 2010) in the Pre-Pyrenean zone, or in the salt lakes of La Playa and La Salineta in the Ebro's Basin (González-Sampériz et al., 2008). Interestingly, this increase in humidity occurred at the end of the IRHP a wet period in the west Mediterranean region, and not at the beginning as in southern Spain (Zoñar Lake, Martín – Puertas et al., 2008). Local hydrogeological factors or a regional variability in moisture availability in Iberian Peninsula during the IRHP could explain this N-S variability.

Episode II: Rise of water levels during the Dark Ages (DA, 500 to 900 cal. yr AD), and lowering of lake levels with increase in detritic input during the Medieval Climate Anomaly (MCA), from 900 to 1400 cal. yr AD

Deposition of homogenous, fine sediments suggests higher lake levels during the first part of the medieval period (Dark Ages). Higher clastic input during this period occurred not only in La Parra, but also in La Cruz Lake (Julià et al., 1998). Higher clastic input could be related to the strong human impact associated to the frequent wars between the Muslims and the Christians (Reconquest) and the emergence of the livestock breeding ("Mesta") lands with frequent burning practises to clear vegetation to increase grassland for pastures (Julià et al., 1998). The presence of coarse facies during this period is indicative of lowered lake levels, as occurs in Lagunillo del Tejo, where periods (López-Blanco et al., 2011) of slightly lower lake levels around 1150 and 1250 AD, and particularly low levels around AD 1400 have been identified.

Episode III: High lake levels and development of meromictic conditions during the Little Ice Age (LIA), from 1400 to 1800 cal. yr. AD.

This period is characterised by generally higher lake levels and lower salinity waters in

all the Torcas (Lagunillo del Tejo, La Cruz, La Parra). Deposition of laminated facies in La Parra is indicative of higher lake levels and likely a reflection of higher effective moisture. However, some anthropogenic effects may have played a significant role. The development of anoxic conditions in La Cruz with consequent deposition of laminated facies with endogenic calcite have been explained by changing farming practices (Julià et al., 1998), with the full development of nomadic livestock breeding or transhumance ("Mesta"). A sparse vegetation cover would favour the rise of the water level in the lake, due to the decrease of plant evapotranspiration. Historical sources (Klein, 1994) indicate that seasonal transhumance or "Mesta" was widespread all over the Cuenca territory during the XVIth century, reaching a maximum from 1500 to 1550 AD, when more than 3 million head of cattle were recorded.

Higher lake levels in Lake La Parra contrast with the low lake levels of Lagunillo del Tejo around 1550-1600 AD (López-Blanco et al., 2011). Based on the macrofossil data and historical record, these authors considered that the sixteenth century was locally very dry. The different hydrology and bathymetry of La Parra (17 m water depth) and El Lagunillo del Tejo (7 m water depth) could be responsible for different sensitivities to hydrological changes. The relatively shallow depth of El Lagunillo de El Tejo could have amplified the environmental changes during the LIA.

The 1760-1800 period coincident with the Malda anomaly (Barriendos y Llasat, 2003) is characterized by major climatic fluctuations, with rapid succession of droughts and floods (Romero-Viana et al., 2010). Nevertheless, from the middle of the eighteenth century, both lakes recorded successively lower lake levels, coinciding with important droughts in both northern and southern Spain around 1750 AD (López-Blanco et al., 2011). The end of the LIA is characterized in La Parra as a period of relatively lower lake levels with deposition of coarser facies.

Episode IV: Relatively high lake levels from 1800 to 2010 cal. yr. AD.

During this period, the lake level is generally high, with some minor episodes of lower levels, coincident with the drought at the beginning of the 20th century (López-Blanco et al., 2011). Later, fine facies and depositional sub-environments are similar to the present-day distribution. Clastic input from the watershed is relatively high, and carbonate production is restricted to the epiliminion and the littoral areas.

Up to the mid 20th century, a demographic increase occurs, with increased agricultural pressure in the watershed, and even the use of some terraces in the Lagunillo del Tejo basin at the beginning of the twentieth century (López-Blanco et al., 2011). Increase in some heavy metals in La Parra sequence, could be related to higher anthropogenic pressure during the late 19th and mid 20th centuries.

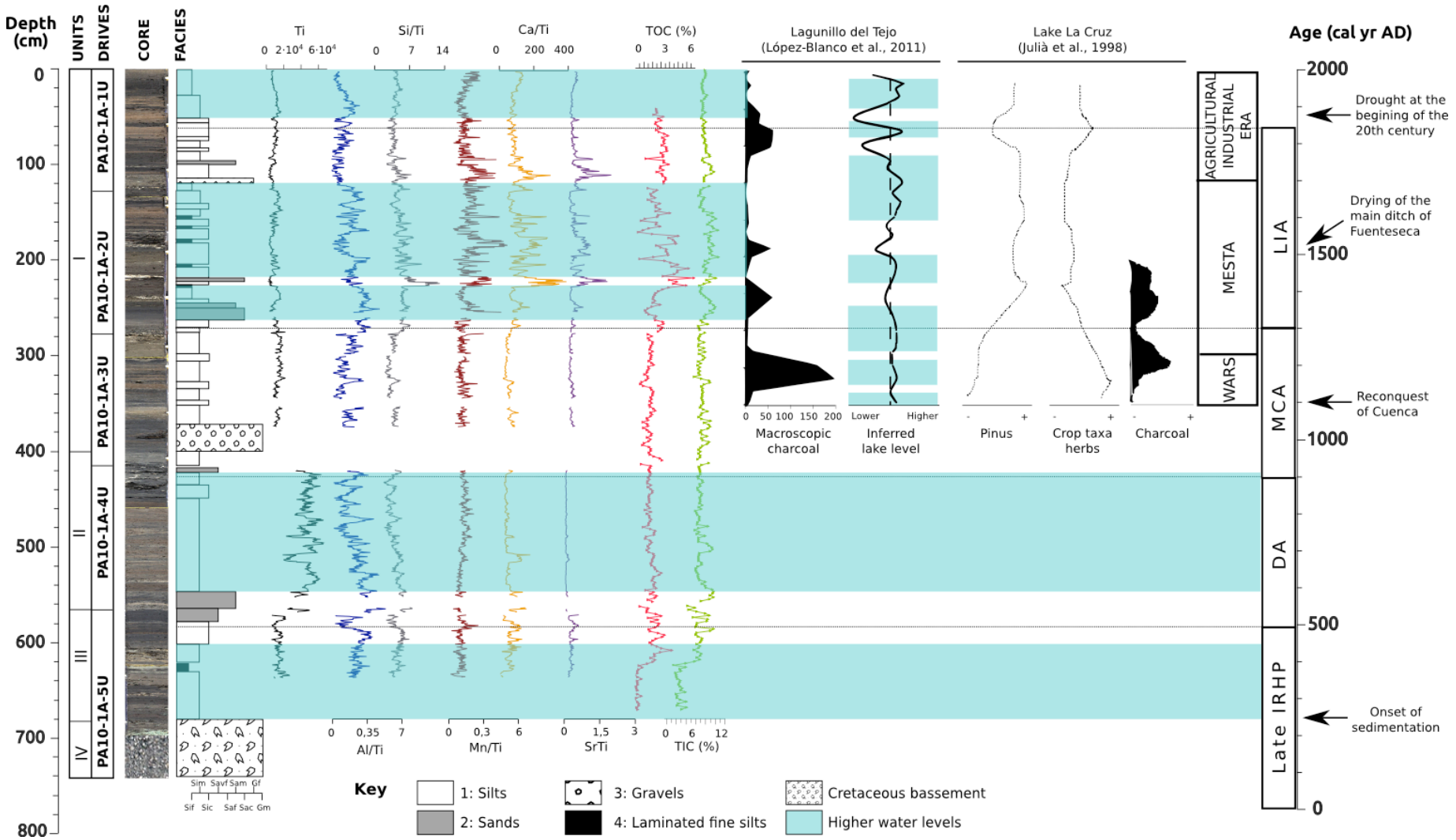

Fig. 18: Compilation of the macrocharcoal record and lake-level reconstruction from Lagunillo del Tejo (first right sub-panel, López-Blanco et al., 2011), synthetic pollen and charcoal records from Lake La Cruz (second right sub-panel, Julià et al., 1998) and principal socio-economic and climatic changes; compared with the stratigraphic profile of Lake La Parra, the periods of higher water levels, and the main geochemical indicators

Climate and paleohydrology in the Iberian Peninsula

The number of extant lakes in Spain is relatively small, compared with other countries, but they occur in a variety of geographic, climatic and ecologic settings (Valero-Garcés and Moreno, 2011). The dominance of semi-arid conditions at present day in a large part of the Iberian Peninsula makes this region very sensitive to hydrological and climatic variations. The intense water management during its long history of human occupation highlights the decisive role of hydrological resources. A number of studies in lakes have been carried out in the Iberian Peninsula to provide reconstructions of past climatic changes to understand the climate mechanisms and the hydrological impacts, as summarised in Moreno et al. (2011).

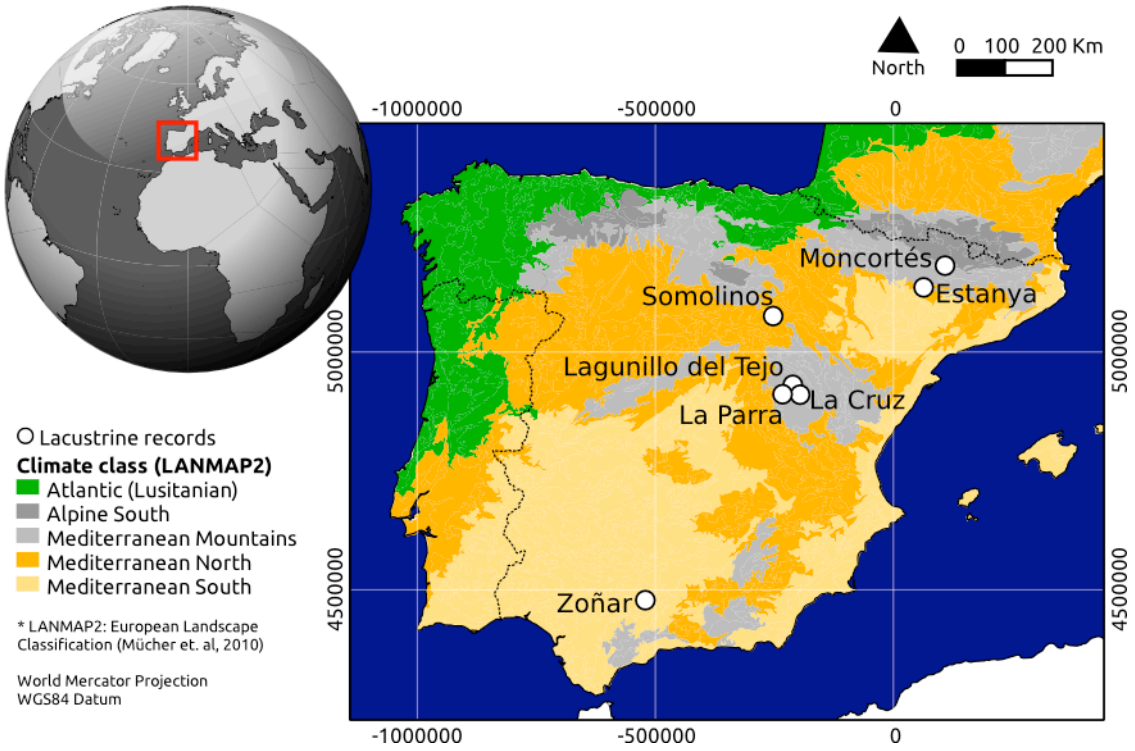

Fig. 19: Location of other lacustrine records used for comparison: in the North of Spain, Moncortés and Estanya; Centre of the Peninsula, Somolinos, La Cruz and Lagunillo del Tejo; and in the South of Spain, Zoñar lake.

Two Pre-Pyrenean Spanish lake records (Northern Spain, Fig. 19), Moncortès and Estanya show good correlation with main climatic changes reconstructed for the last 1600 years in Lake La Parra.

In Moncortès lake, (Corella et al., 2010) warmer temperatures and arid conditions have been suggested during the MCA (1000-1300 AD), coinciding with a period of high clastic input; while the LIA (1330-1840 AD) marks an episode of lower clastic input (low magnetic susceptibility) occurred during wetter climatic conditions and likely decrease anthropic pressure in the watershed.

At nearby brackish karstic Estanya lake, shallower water levels and saline conditions predominated during medieval times (870-1300 AD), and generally higher lake levels and more diluted waters during the LIA (1300-1900 AD), althought this period shows a complex pattern of wet and arid intervals (Morellón et al., 2009). Maximum lake levels occurred during the nineteenth century, and declined during the twentieth century.

Inside Las Torcas Lake Complex (Middle-East Spain, Fig. 19), La Cruz lake record (Julià et al., 1998) shows lower lake levels during the ninth-eleventh centuries (Medieval

ages), indicative of drier conditions. Later, the development of meromictic conditions during the LIA is related to synergetic effects of colder temperatures and higher lake levels, suggesting wetter conditions. This pattern is similar to La Parra Lake.

In Central Spain, between Tajo and Duero basins (Fig. 19), higher water levels have been also reported at Somolinos tufa lake (Currás et al., 2012), during the Late Roman Period, as suggested by the disappearance of benthic diatoms and a reduction in molluscs populations. Later, the marked increase in the proportion of facultative planktonic and benthic diatoms provides strong evidence for lake shallowing, suggesting a decline in lake levels after 370 AD, coinciding with the drop of water levels in Lake La Parra between 400-500 AD.

In southern Spain, sedimentological data from Zoñar lake (Fig. 19, Martín-Puertas et al., 2008) presents a varved interval deposited during the Iberian-Roman ages (550 BC-AD 350), with similarities with the short fine-laminated interval showed in La Parra record around 350-400 AD, although it includes an arid interval during the Roman Imperial Epoch (190 BC-AD 150). Then, from 300 BC to 600 AD, includes the most humid conditions of the last three millennia in southern Spain. Later, the record indicates arid conditions synchronous with the MCA and two humid periods between 1200 and 1400 AD and around 1600 AD during the LIA, consistent with La Parra record interpretation.

Regional implications

The paleohydrological and paleoenvironmental fluctuations reconstructed from Lake La Parra are coherent with other lacustrine records of the Iberian Peninsula (Fig. 20) showing overall agreement since 900 AD, giving confidence that they reflect common climatic forcing. In general, Iberian lakes show lower water levels and higher salinities during the 11th to 13th centuries, synchronous with the MCA. On the other hand, during the LIA (15th to 19th centuries) more humid conditions and higher lake levels have been reconstructed. This pattern is confirmed by other lake, marine and tree-rings records from Iberia and Morocco (Moreno et al., 2011)

In contrast, some lakes of the eastern Mediterranean show an opposite pattern of wet MCA and dry LIA (Roberts et al., 2012) (Fig. 20), reflecting an anti-phase relationship in precipitation and atmospheric pressure with the western Mediterranean. Then, Lake La Parra provides additional paleolimnological evidence for an east-west climate see-saw pattern in the Mediterranean for the MCA and the LIA, enforcing the hypothesis of an east-west climate anti-phase in this region since 900 AD.

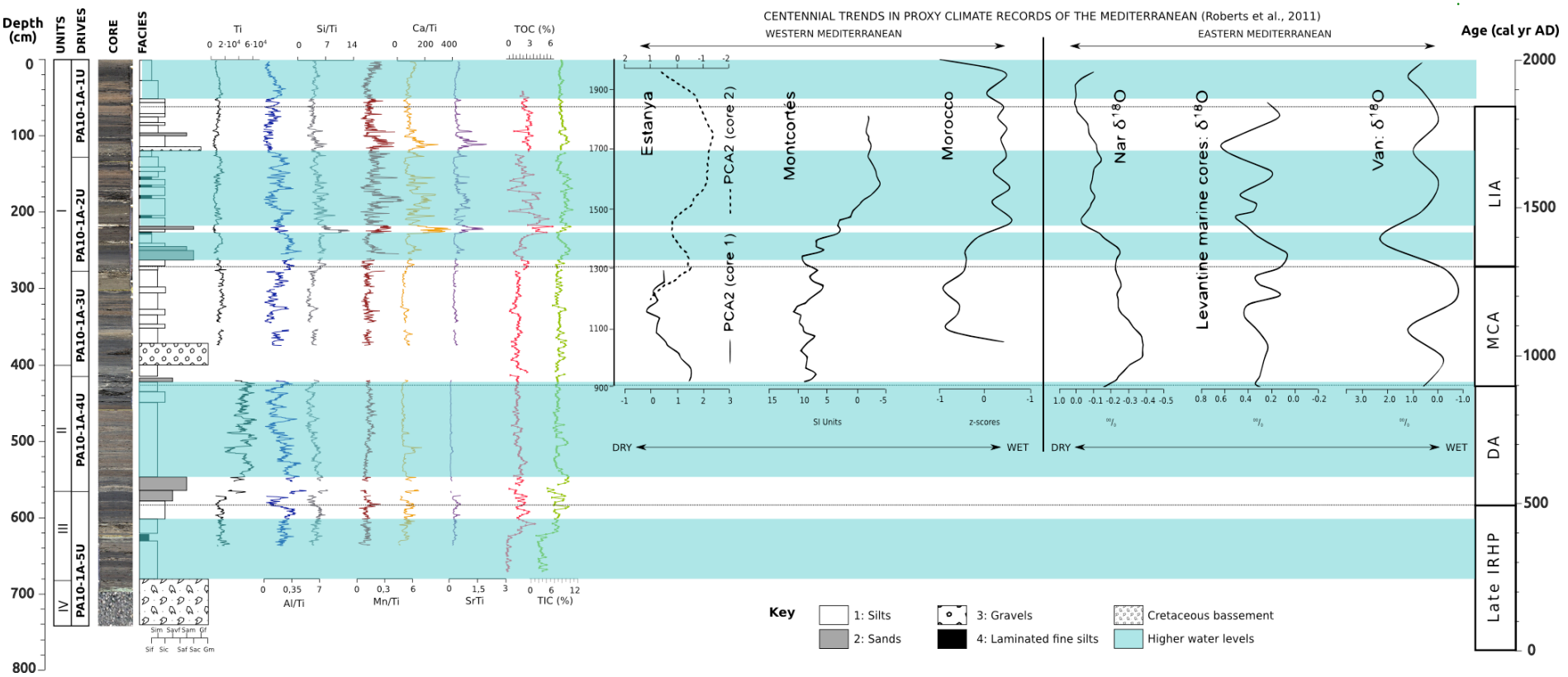

Fig. 20: Centennial trends in proxy climate records (Roberts et al., 2012) compared with the main geochemical proxies of Lake La Parra record. High water levels are represented in blue. First right subpanel - Western Mediterranean: Moncortés magnetic susceptibility, Estanya PCA axis 2 and Moroccan tree ring data. Second right subpanel – Eastern Mediterranean: $\partial^{18}O$ for Nar and Van lakes and Levantine marine cores

Conclusions

The sedimentary record of Lake La Parra constitutes the longest (6,93 m, last 1600 years) and more accurately dated record (nine radiocarbon AMS samples) of Las Torcas Lake Complex. The sedimentary and hydrologic reconstruction based on sedimentological, geochemical and mineralogical analysis has allowed identification of four main lithostratigraphical units and five main paleohydrologic episodes during the Late Holocene.

Four main depositional sub-environments have been described based on the spatial distribution of sedimentary facies in Lake La Parra: (i) the littoral platform; (ii) the talus area; (iii) the offshore transitional area; and (iv) the offshore distal area. The distribution of these sub-environments is controlled strongly by lake bathymetry that today exerts a key influence on the depositional conditions.

The sedimentary sequence of Lake La Parra is mainly constituted by clastic carbonated sediments and it is characterized by a high variability of sedimentary facies, mainly controlled by changes in the detritic input and hydrological variability along the last 1600 years. The onset of lacustrine sedimentation around 250 yr AD demonstrates a rise of the water levels that changed the hydrogeology of the basin from a “dry” to a “flooded” torca. The dominance of fine clastic homogeneous sedimentation before the 8th century (Dark Ages) suggests a period of relatively high lake levels. Deposition of relatively coarser clastic facies during the late Middle Ages is interpreted as a decrease in lake levels synchronous to the Medieval Climate Anomaly (900-1400 AD) and the impact of increased human activities in the region to increase grassland for pastures with the emergence of “Mesta”, the livestock breeding transhumance. The deposition of fine silts and the presence of fine-laminated facies, which reflect a trend to more frequent anoxia in the bottom of the lake, are coherent with higher lake levels during the Little Ice Age (1400-1800 AD). More recently, a slight lowering of water levels is indicated by deposition of coarser facies around 1900 AD. Deposition during the last century is dominated by fine silts facies.

The increase of detrital input in Lake La Parra during the Middle Ages is in agreement with the effect of socio-economic transformations and climate change observed in nearby Lagunillo del Tejo (López-Blanco et al., 2011) and Lake La Cruz (Julià et al., 1998). The main socio-economic land use changes were the woodland clearance to increase grassland for pastures during the 16th century. However, the geographical situation and climate conditions limited the land management either during past and present to forest exploitation, pastures and small areas of cereals and subsistence agriculture, without excessive modification of the natural environment (Romero-Viana et al., 2010). Although the lakes and watersheds are protected, currently, the local karstic aquifer feeding the lake complex is being exploited for irrigation.

The paleohydrological and paleoenvironmental fluctuations of Lake La Parra can be correlated with other lacustrine records of the Iberian Peninsula. The main climate and hydrological episodes recorded in La Parra are coherent with available Iberian records. Especially relevant are: i) the synchronicity of the Iberian-Roman Humid Period (300-500 AD) with the presence of fine-laminated sediments, indicating a wetter episode with high lake-levels of regional significance although with large regional variability, ii) the occurrence of shallower lake levels during a drier phase corresponding with the Medieval Climatic Anomaly; and iii) the development of laminated facies with endogenic carbonates from 1450 to 1650 AD, coincident with the Little Ice Age and suggestive of higher lake

levels although with a large climate and hydrological variability. The La Parra record provides additional data to the paleoclimate reconstructions for the last 2000 years in the Iberian Peninsula (Moreno et al., 2012) and further support to the hypothesis of Roberts et al. (2012) of an east-west climate see-saw in the Mediterranean region since 900 AD.

References

Alley, R.B., Mayewski, P.A., Sowers, T., Stuiver, M., Taylor, K.C., Clark, P.U., 1997. Holocene climatic instability: A prominent, widespread event 8200 yr ago. Geology 25, 483.

Alonso, F., 1986. Karst Externo. Las torcas de Cuenca, in: E. Martínez de Pistón, Tello, B. (Eds.), Atlas De Geomorfología. Alianza, Madrid, pp. 273–284.

Barreiro-Lostres, F., Moreno, A., Valero-Garcés, B., 2011. Facies sedimentarias de la laguna kárstica de La Parra (Cuenca) durante los últimos 1600 años cal. BP. Geogaceta 50, 109–112.

Barriendos, M., Llasat, M.C., 2003. The case of the "Maldá" anomaly in the Western Mediterranean basin (AD 1760-1800): An example of a strong climatic variability. Clim. Change 61, 191–216.

Batist, M., Chapron, E., 2008. Lake systems: Sedimentary archives of climate change and tectonics. Palaeogeography, Palaeoclimatology, Palaeoecology 259, 93–95.

Brauer, A., 2004. Annually laminated lake sediments and their palaeoclimatic relevance, in: Fischer, H., Kumke, T., Lohmann, G., Floser, G., Miller, H., Von Storch, V., Negendank, J.F.W. (Eds.), The Climate in Historical Times. Towards a Synthesis of Holocene Proxy Data and Climate Models. Springer, pp. 109–129.

Carmona,, J.M., Bitzer, K, 2001. Los sistemas cársticos de Lagunas de Cañada del Hoyo y Torcas de los Palancares (Serranía de Cuenca. españa), in: Las Caras Del Agua Subterránea. UniZar D 26-35/1, pp. 451–460.

Chung, F.H., 1975. Quantitative interpretation of X-ray diffraction patterns of mixtures. III. Simultaneous determination of a set of reference intensities. Journal of Applied Crystallography 8, 17–19.

Cohen, A.S., 2003. Paleolimnology the history and evolution of lake systems. New York : Oxford University Press, Oxford.

Corella, J.P., Amrani, A.E., Sigró, J., Morellón, M., Rico, E., Valero-Garcés, B.L., 2010. Recent evolution of Lake Arreo, northern Spain: influences of land use change and climate. Journal of Paleolimnology 46, 469–485.

Corella, J.P., Moreno, A., Morellón, M., Rull, V., Giralt, S., Rico, M.T., Pérez-Sanz, A., Valero-Garcés, B.L., 2010. Climate and human impact on a meromictic lake during the last 6,000 years (Montcortès Lake, Central Pyrenees, Spain). Journal of Paleolimnology 46, 351–367.

Crowley, T.J., 2000. Causes of Climate Change Over the Past 1000 Years. Science 289, 270–277.

Currás, A., Zamora, L., Reed, J.M., García-Soto, E., Ferrero, S., Armengol, X., Mezquita-Joanes, F., Marqués, M.A., Riera, S., Julià, R., 2012. Climate change and human impact in central Spain during Roman times: High-resolution multi-proxy analysis of a tufa lake record (Somolinos, 1280m asl). CATENA 89, 31–53.

Custodio, Llamas, 1996. Hidrología subterránea, 2º ed. Omega.

Duplessy, J., 2005. Les accidents climatiques brutaux et localisés et leurs conséquences. Comptes Rendus Geosciences 337, 881–887.

Eraso, A.E., López-Acevedo, V., López, M., Navarro, V., Suso, J., Santos, V., 1979. Estudio De Las Torcas De Palancares Y Cañada Del Hoyo En El Karst De La Serranía De Cuenca, 1979th ed, Kobie. Bilbao.

Escuder, R., Fralie, J., Salvador, J., Ribera, Fi., Sánchez-Vila, X., Vázquez-Suñé, E. (Eds.), 2009. Hidrogeología. Conceptos básicos de Hidrogeología suterránea. FCIHS, Barcelona.

Escudero, A., Regato, P., 1992. Ordenación de la vegetación de las torcas de la Serranía de Cuenca y sus relaciones con algunos factores del medio. Orsis 7, 41–55.

González-Sampériz, P., Valero-Garcés, B.L., Moreno, A., Morellón, M., Navas, A., Machín, J., Delgado-Huertas, A., 2008. Vegetation changes and hydrological fluctuations in the Central Ebro Basin (NE Spain) since the Late Glacial period: Saline lake records. Palaeogeography, Palaeoclimatology, Palaeoecology 259, 157–181.

Hegerl, G., Luterbacher, J., Gonzalez-Rouco, F., Tett, S.F.B., Crowley, T., Xoplaki, E., 2011. Influence of human and natural forcing on European seasonal temperatures. Nature Geosci 4, 99–103.

Houghton, J., 2001. The science of global warming. Interdisciplinary Science Reviews 26, 247–257.

Julia, R, Burjachs, F, Dasi, MJ, Mezquita, F, Miracle, MR, Roca, JR, Seret, G, Vicente, E, 1998. Meromixis origin and recent trophic evolution in the Spanish mountain lake La Cruz. AQUATIC SCIENCES 60, 279–299.

Klein, J., 1994. La Mesta: estudio de la historia económica española 1273 – 1836. Alianza Editorial (Alianza Universidad), Barcelona.

Kylander, M.E., Ampel, L., Wohlfarth, B., Veres, D., 2011. High-resolution X-ray fluorescence core scanning analysis of Les Echets (France) sedimentary sequence: new insights from chemical proxies. J. Quaternary Sci. 26, 109–117.

López-Blanco, C., Gaillard, M.-J., Miracle, M.R., Vicente, E., 2011. Lake-level changes and fire history at Lagunillo del Tejo (Spain) during the last millennium: Climate or humans? The Holocene 22, 551–560.

Mann, M.E., 2007. Climate Over the Past Two Millennia. Annu. Rev. Earth Planet. Sci. 35, 111–136.

Martín Puertas, C.-P., 2008. Arid and humid phases in southern Spain during the last 4000 years: The Zoñar Lake record, Córdoba. Holocene 18, 907–921.

Martín-Puertas, C., Valero-Garcés, B.L., Brauer, A., Mata, M.P., Delgado-Huertas, A., Dulski, P., 2009. The Iberian–Roman Humid Period (2600–1600 cal yr BP) in the Zoñar Lake varve record (Andalucía, southern Spain). Quaternary Research 71, 108–120.

Martín-Puertas, C., Valero-Garcés, B.L., Mata, M.P., Moreno, A., Giralt, S., Martínez-Ruiz, F., Jiménez-Espejo, F., 2009. Geochemical processes in a Mediterranean Lake: a high-resolution study of the last 4,000 years in Zoñar Lake, southern Spain. Journal of Paleolimnology 46, 405–421.

Mateo Gutiérrez Elorza, Valverde, 1994. El sistema de poljes del río Guadazaón (Cordillera Ibérica, prov. de Cuenca). Cuaternario y Geomorfología 8, 87–95.

Morellón, M., Valero-GarcéS, B., Anselmetti, F., Ariztegui, D., Schnellmann, M., Moreno, A., Mata, P., Rico, M., Corella, J.P., 2009. Late Quaternary deposition and facies model for karstic Lake Estanya (North-eastern Spain). Sedimentology 56, 1505–1534.

Morellón, M., Valero-Garcés, B., González-Sampériz, P., Vegas-Vilarrúbia, T., Rubio, E., Rieradevall, M., Delgado-Huertas, A., Mata, P., Romero, Ó., Engstrom, D.R., López-Vicente, M., Navas, A., Soto, J., 2009a. Climate changes and human activities recorded in the sediments of Lake Estanya (NE Spain) during the Medieval Warm Period and Little Ice Age. Journal of Paleolimnology 46, 423–452.

Morellón, M., Valero-Garcés, B., González-Sampériz, P., Vegas-Vilarrúbia, T., Rubio, E., Rieradevall, M., Delgado-Huertas, A., Mata, P., Romero, Ó., Engstrom, D.R., López-Vicente, M., Navas, A., Soto, J., 2009b. Climate changes and human activities recorded in the sediments of Lake Estanya (NE Spain) during the Medieval Warm Period and Little Ice Age. Journal of Paleolimnology 46, 423–452.

Moreno, A., Giralt, S., Valerogarces, B., Saez, A., Bao, R., Prego, R., Pueyo, J., Gonzalezsamperiz, P., Taberner, C., 2007. A 14kyr record of the tropical Andes: The Lago Chungará sequence (18°S, northern Chilean Altiplano). Quaternary International 161, 4–21.

Moreno, A., González-Sampériz, P., Morellón, M., Valero-Garcés, B.L., Fletcher, W.J., 2010. Northern Iberian abrupt climate change dynamics during the last glacial cycle: A view from lacustrine sediments. Quaternary Science Reviews.

Moreno, A., González-Sampériz, P., Morellón, M., Valero-Garcés, B.L., Fletcher, W.J., 2012. Northern Iberian abrupt climate change dynamics during the last glacial cycle: A view from lacustrine sediments. Quaternary Science Reviews 36, 139–153.

Moreno, A., Mario Morellón, Ccelia Martín-PuertAs, Jaime Frigola, Miguel Canals, Isabel Cacho, Juan-Pablo Corella, Ana Pérez, Ánchel Belmonte, Teresa Vegas-Vilarrúbia, Penélope González-Sampériz, Blas Valero-Garcés, 2011. Was there a common

hydrological pattern in the Iberian Peninsula region during the Medieval Climate Anomaly? PAGES News 19, 16–18.
Peña, J.L., Lozano, M.V., 2004. LAS UNIDADES DEL RELIEVE ARAGONÉS, in: Longares, L.A., Sánchez, M. (Eds.), Geografía Física De Aragón. Aspectos Generales y Temáticos. Universidad de Zaragoza e Institución Fernando el Católico, pp. 3–14.
Reimer, P.J., Baillie, M.G.L., Bard, E., Bayliss, A., Beck, J.W., Blackwell, P.G., Bronk-Ramsey, C., 2009. INTCAL 09 and MARINE09 aadiocarbon age calibration curves, 0-50,000 years Cal BP. Radiocarbon 51, 1111–1150.
Richter, T.O., van der Gaast, S., Koster, B., Vaars, A., Gieles, R., de Stigter, H.C., De Haas, H., van Weering, T.C.E., 2006. The Avaatech XRF Core Scanner: technical description and applications to NE Atlantic sediments. Geological Society, London, Special Publications 267, 39–50.
Roberts, N., Moreno, A., Valero-Garcés, B.L., Corella, J.P., Jones, M., Allcock, S., Woodbridge, J., Morellón, M., Luterbacher, J., Xoplaki, E., Türkeş, M., 2012. Palaeolimnological evidence for an east–west climate see-saw in the Mediterranean since AD 900. Global and Planetary Change.
Rodrigo, MA, Miracle, MR, Vicente, E, 2001. The meromictic Lake La Cruz (Central Spain). Patterns of stratification. AQUATIC SCIENCES 63, 406–416.
Romero, L., Camacho, A., Vicente, E., Miracle, M.R., 2006. Sedimentation Patterns of Photosynthetic Bacteria Based on Pigment Markers in Meromictic Lake La Cruz (Spain): Paleolimnological Implications. J Paleolimnol 35, 167–177.
Romero-Viana, L., Julià, R., Camacho, A., Vicente, E., Miracle, M.R., 2008. Climate Signal in Varve Thickness: Lake La Cruz (spain), a Case Study. J Paleolimnol 40, 703–714.
Romero-Viana, L., Julià, R., Schimmel, M., Camacho, A., Vicente, E., Miracle, M.R., 2011. Reconstruction of annual winter rainfall since A.D.1579 in central-eastern Spain based on calcite laminated sediment from Lake La Cruz. Climatic Change.
Romero-Viana, L., Keely, B.J., Camacho, A., Vicente, E., Miracle, M.R., 2009. Primary production in Lake La Cruz (Spain) over the last four centuries: reconstruction based on sedimentary signal of photosynthetic pigments. J Paleolimnol 43, 771–786.
Segura, M., García, A., Carenas, B., Calonge, A., 1988. Unidades estratigraficas en el Cretacico medio de la región Cuenca-Atienza (Cordillera Ibérica). Geologica Acta 23, 291–298.
Stuiver, M., Reimer, P.J., 1993. CALIB's user guide rev. 3.0. University of Washington, Quaternary Isotope Laboratory.
Tjallingii, R., 2006. Application and quality of X-Ray Fluorescence core scanning in reconstructing late Pleistocene NW African continental margin sedimentation patterns and paleoclimate variations.
Tjallingii, R., Y. Hamann, D. Garbe-Schönberg, G. Jan Weltje, U. Röhl, workshop participants, 2011. 2010 international workshop on XRF core scanning Texel, The Netherlands, 8-10 September 2010. PAGES News 19, 90–91.
Turney, C.S.M., Baillie, M., Palmer, J., Brown, D., 2006. Holocene climatic change and past Irish societal response. Journal of Archaeological Science 33, 34–38.
Valero-Garcés, B.L., Moreno, A., 2011. Iberian lacustrine sediment records: responses to past and recent global changes in the Mediterranean region. Journal of Paleolimnology 46, 319–325.